Molecular Biology Reports (2026) 53:727
https://doi.org/10.1007/s11033-026-11899-4

ORIGINAL ARTICLE

Neuroprotective effects of black elderberry (*Sambucus nigra*) extract through the role of miR-124-5p and miR-144-5p in a streptozotocin-induced Type 2 diabetic rat model

Arzu Gezer[1,2] · Fatma Sanlı[3,7] · Haktan Aslan[4] · Mustafa Özkaraca[5] · Nurcan Kılıç Baygutalp[4] · Ebru Karadağ Sarı[6] · Omer Faruk Karatas[3,7] · Hilal Üstündağ[8]

Received: 23 January 2026 / Accepted: 29 April 2026
© The Author(s), under exclusive licence to Springer Nature B.V. 2026

Abstract

Background Type 2 diabetes mellitus (T2DM) leads to neurological complications through multiple pathways. Black elderberry (*Sambucus nigra*, SN) is rich in bioactive compounds with potential neuroprotective properties. This study sought to evaluate the neural-protective potential of SN extract in STZ-diabetic rats using an integrated molecular, biochemical, and histomorphological approach.

Methods Forty male *Sprague-Dawley* rats were divided into four groups ($n=10$/group): control (C; 0.9% NaCl), SN (0.040 g/kg body weight), diabetes mellitus (DM; streptozotocin 50 mg/kg), and DM + SN (streptozotocin + SN). The treatment period was 10 weeks. Brain tissue was analyzed for histopathological changes, caspase-3 expression, microRNA (miRNA) expression, and oxidative stress markers.

Results Histopathological examination revealed severe neuronal degeneration in the DM group, significantly attenuated in the DM + SN group ($p<0.001$). Caspase-3 immunoreactivity was markedly increased in DM group compared to controls and significantly reduced by SN treatment ($p<0.01$). In situ hybridization showed high ribonucleic acid (rno)-miR-124-5p and rno-miR-144-5p expression in C and SN groups, with reduced expression in DM group ($p<0.05$). SN treatment moderated these changes in DM + SN group. Quantitative real-time polymerase chain reaction (qRT-PCR) confirmed decreased miR-124 expression in DM group, restored to control levels by SN treatment. Biochemically, SN extract reversed diabetes-induced changes in oxidative stress markers, decreasing malondialdehyde (MDA) levels while increasing glutathione (GSH) and nitric oxide synthase (NOS) levels ($p<0.01$).

Conclusions SN extract exerted robust neuroprotective actions in the diabetic brain through apoptosis inhibition, miRNA profile restoration, and amelioration of redox imbalance, underscoring its therapeutic promise for diabetes-associated neuropathy.

Keywords Antioxidant · Black elderberry · Brain · Diabetes · *In situ* hybridization · miR-124 · miR-144

✉ Arzu Gezer
arzu.gezer@atauni.edu.tr

✉ Hilal Üstündağ
hilal.ustundag@erzincan.edu.tr

[1] Vocational School of Health Services, Atatürk University, Erzurum, Türkiye, Turkey

[2] Pharmaceutical Research and Development, Graduate School of Natural and Applied Sciences, Atatürk University, Erzurum, Türkiye, Turkey

[3] Department of Molecular Biology and Genetics, Faculty of Science, Erzurum Technical University, Erzurum, Türkiye, Turkey

[4] Department of Biochemistry, Faculty of Pharmacy, Atatürk University, Erzurum, Türkiye, Turkey

[5] Department of Pathology, Faculty of Veterinary Medicine, Cumhuriyet University, Sivas, Türkiye, Turkey

[6] Department of Histology and Embryology, Faculty of Veterinary Medicine, Kafkas University, Kars, Türkiye, Turkey

[7] Molecular Cancer Biology Laboratory, High Technology Application and Research Center, Erzurum Technical University, Erzurum, Türkiye, Turkey

[8] Department of Physiology, Faculty of Medicine, Erzincan Binali Yıldırım University, Erzincan, Türkiye, Turkey

Published online: 08 May 2026

Background

Type 2 diabetes mellitus (T2DM), which accounts for over 90% of all diabetes cases, has become a major public health crisis with an escalating global burden. According to the 11th edition of the International Diabetes Federation (IDF) Diabetes Atlas, approximately 589 million adults (aged 20–79 years) worldwide were living with diabetes in 2024, corresponding to a prevalence of 11.1%, and this number is projected to rise to 853 million by 2050 [1]. In Türkiye, the situation is particularly alarming, as the country has the highest diabetes prevalence in the European region, estimated at approximately 16.5% among adults [2, 3]. T2DM, through both its immediate metabolic derangements and long-term organ damage, diminishes patient well-being and imposes a substantial socioeconomic burden. When glycemic regulation remains suboptimal in T2DM or when antidiabetic therapy proves inadequate, susceptibility to macrovascular disorders (coronary atherosclerosis, peripheral arterial compromise, hypertensive disease, cerebrovascular accidents) and microvascular pathologies (renal impairment, peripheral nerve dysfunction, retinal deterioration) escalates substantially [4]. Therefore, preventive measures before the onset of T2DM can reduce both the frequency of disease occurrence and the related morbidity and mortality.

The frequency of certain new complications increases, particularly in elderly diabetic patients. Numerous studies have shown that T2DM hastens cerebral senescence and cognitive deterioration while amplifying dementia susceptibility, a concern of mounting relevance given demographic aging trends [5]. Oxidative stress associated with T2DM and insulin resistance leads to harmful effects of reactive oxygen species on lipids, proteins, and DNA, contributing to neuronal damage and the formation of segmental demyelination in diabetic patients [6, 7]. It has been shown that with increasing age, the influence of T2DM on cerebral vascular and neurodegenerative issues increases, which can ultimately lead to subcortical infarcts, white and gray matter lesions, and cerebral microbleeds. Reductions in total brain volume alongside gray and white matter atrophy serve as neuroimaging indices of both diffuse and region-specific cerebral degeneration [8].

The management of T2DM and its complications has increasingly drawn attention toward plant-derived therapeutic agents. Botanical remedies have a centuries-long tradition in addressing metabolic ailments, and the bioactive constituents they contain—particularly polyphenols, flavonoids, and anthocyanins—have demonstrated notable antioxidant, anti-inflammatory, and antidiabetic properties [9]. These natural compounds exert their protective effects by scavenging reactive oxygen species, modulating key signaling pathways, and attenuating inflammatory cascades, thereby offering a complementary approach to conventional pharmacotherapy. Among these medicinal plants, black elderberry (*Sambucus nigra*, SN) has gained considerable interest due to its particularly rich content of anthocyanins and polyphenolic compounds with potent biological activities [10].

Sambucus nigra has long been recognized as a versatile medicinal plant with applications spanning traditional and contemporary healthcare practices. Native to various temperate regions, including the Northern Anatolian zone of Türkiye, this species thrives in bushy habitats. Virtually every anatomical structure of the plant—from root to fruit—has been attributed therapeutic significance [11]. The phytochemical profile of SN is notably enriched with anthocyanins, diverse polyphenols, and flavonoids that contribute to its marked antioxidant capacity. Domínguez et al. [12] conducted a detailed LC-MS/MS-based profiling of elderberry nutritional and polyphenolic composition, revealing an abundant reservoir of aromatic hydroxylated phenolics. Their analysis detected multiple phenolic acid species (gallic, gentisic, 4-hydroxybenzoic, caffeic, vanillic, coumaric, and ferulic acids) alongside five flavonol derivatives (rutin, quercetin, kaempferol, syringetin, isorhamnetin) and the anthocyanin malvidin [12]. Collectively, these phytoconstituents exhibit a broad spectrum of pharmacological activities encompassing anti-inflammatory, free radical–scavenging, antiviral, antineoplastic, and glucose-regulatory properties [10]. It has been proven that SN increases bone mineral density and enhances insulin secretion from the pancreas β cells. Additionally, it has been reported that SN acts as a free radical scavenger, reducing oxidative stress in diabetic rat models [13]. In addition to its antihyperglycemic effect, SN has been found to be effective in reducing neuropathic pain, a long-term complication of T2DM [14]. Beyond polyphenols, SN harbors functionally distinct macromolecules such as ribosome-inactivating proteins and lectins. The former class disrupts ribosomal translation machinery by catalyzing depurination of rRNA through their intrinsic N-glycosidase activity [15]. Given these characteristics, SN extract could be considered as a potential source of bioactive compounds for formulations aimed at adjuvant therapy in T2DM.

MicroRNAs (miRNAs) constitute a class of small non-coding RNA molecules that govern post-transcriptional gene silencing. Through complementary sequence recognition of target messenger RNAs (mRNAs), miRNAs trigger either transcript destabilization or translational arrest [16]. T2DM patients have increased risk for multiple comorbidities including cardiovascular disease, hypertension, depression, and Alzheimer's disease [17]. In this context, miR-124-5p, predominantly expressed in brain tissue, plays crucial roles in neuronal development and has been shown dysregulated in diabetic conditions, affecting insulin secretion and glucose

metabolism [6, 18]. Similarly, miR-144-5p has been identified as a key regulator in both diabetes and neurological disorders, with elevated levels observed in diabetes patients and significant effects on oxidative stress responses [19, 20]. The involvement of these miRNAs in both diabetic and neurological pathways, particularly in T2DM and Alzheimer's disease progression, suggests shared molecular pathways in these conditions and makes them potential therapeutic targets for diabetes-induced neural complications [21, 22].

Therefore, this study aimed to investigate the neuroprotective effects of SN extract in streptozotocin-induced T2DM rats. Given that T2DM-induced chronic hyperglycemia and oxidative stress are key contributors to central nervous system complications, we hypothesized that SN extract, through its rich polyphenolic content, may attenuate diabetes-induced neuronal damage via modulation of oxidative stress, apoptotic signaling, and miRNA expression. The potential therapeutic effects were evaluated through multiple approaches: histopathological examination of neuronal damage, immunohistochemical analysis of caspase-3 expression, molecular assessment of miR-124-5p and miR-144-5p levels, and biochemical measurement of oxidative stress markers including MDA, GSH, and NOS levels in brain tissue.

Methods

Black elderberry (SN) plant extraction

The plant specimen was purchased from Temmuz Organic Production Farm (Konya, Türkiye) (code number: ST00136, and confirmed by Asst. Prof. Leyla Güven. The dried elderberries were ground and subjected to extraction with 50% ethanol under acidic conditions (pH: 2) for a total of 5 days at room temperature in the dark, with shaking maceration repeated three times. The acidified methanol extract was prepared using a 25% HCl: methanol (1:9) solvent mixture, extracted at room temperature and in an ultrasonic bath for 30 min, repeated three times [12]. The solvent was evaporated using a rotary evaporator, and the obtained extracts were lyophilized to dryness using a rotavapor (< 40 °C). The extracts were stored in dark-colored bottles at -20 °C until the time of analysis [23]. The bioactive composition of SN extract, including anthocyanins (malvidin), flavonols (quercetin, rutin, kaempferol), and phenolic acids (gallic, caffeic, ferulic acid), has been extensively characterized in previous studies [12, 15].

Animals and experimental groups

Eight- to ten-week-old male *Sprague Dawley* rats with a body weight (BW) of 200 ± 20 g were used in the study. Sample size was determined using G*Power software (version 3.1.9.7). Based on previous STZ-induced diabetic rat study (Ayan et al., 2019), an effect size of f = 0.56 was calculated. With α = 0.05 and power = 0.80, one-way ANOVA analysis required $n = 10$ per group (total $N = 40$). The study strictly adhered to the ARRIVE guidelines and was conducted following the national regulations for the ethical use and care of laboratory animals. During the experiment, the rats were allowed *ad libitum* access to standard laboratory chow and tap water under a 12-hour dark/light cycle at 22 ± 3 °C.

Rats were randomly divided into four experimental groups ($n = 10$/group):

Control (C): Healthy rats receiving 0.5 mL of 0.9% NaCl via oral gavage every other day for 10 weeks. Rats were not subjected to STZ injection.

Sambucus nigra (SN): Healthy rats receiving SN extract (0.040 g/kg BW) suspended in 0.9% NaCl via oral gavage every other day for 10 weeks. No diabetes induction was performed [24].

Diabetes mellitus (DM): Rats were fasted for 8 h and then received a single intraperitoneal injection of STZ (50 mg/kg BW) in citrate buffer (0.1 M, pH 4.5) to induce diabetes [25]. Blood glucose levels were measured from tail vein samples at 72 h post-injection to confirm diabetes (FBG > 250 mg/dL) and again at week 10 to assess progression without treatment.

Diabetes + Sambucus nigra (DM + SN): Following diabetes confirmation (as above), rats received SN extract (0.040 g/kg BW) via oral gavage starting one day post-diagnosis and continuing every other day for 10 weeks.

Sample collection

Upon completion of the 10-week intervention, animals underwent an 8-hour fast with unrestricted water access before terminal FBG assessment and blood sampling. Deep surgical-plane anesthesia was subsequently achieved via sevoflurane inhalation (Sevorane®, Abbott Laboratories, Istanbul, Türkiye), and euthanasia was performed by overdose of inhalational anesthesia, in accordance with the institutional animal care and use committee guidelines and the AVMA Guidelines for the Euthanasia of Animals. Immediately following euthanasia, trunk blood was drawn into plain collection tubes and permitted to coagulate at ambient temperature over 30 min. Samples were then centrifuged at 1500 × g for 5 min at 4 °C. The resulting serum supernatants were carefully collected, aliquoted, and stored at − 80 °C until biochemical and molecular analyses. Following

decapitation, intact brains were swiftly harvested and rinsed with chilled sterile physiological saline to clear residual blood. A mid-sagittal division yielded two hemispheres: one was flash-frozen in liquid nitrogen and maintained at −80 °C for subsequent biochemical assays and qRT-PCR analyses, while the other hemisphere was immersed in 10% neutral buffered formalin solution for 24–48 h for histopathological examination. Fixed tissues were processed through graded ethanol series, cleared in xylene, and embedded in paraffin blocks for sectioning.

Histopathological examination

Harvested brain specimens underwent fixation in 10% phosphate-buffered formalin, sequential dehydration through graded ethanol concentrations, xylene clearing, and paraffin infiltration. Serial sections of 4 µm-thick sections were obtained and mounted on poly-L-lysine-coated slides. Deparaffinized sections received H&E staining for morphological evaluation. Cortical neuronal degeneration and nuclear pyknosis were graded semi-quantitatively by determining the proportion of damaged neurons across six randomly sampled microscopic fields at ×20 magnification. The grading scale was assigned as follows: Absent (-) designating intact neuronal architecture with uniformly round, vesicular nuclei bearing conspicuous nucleoli. Mild (+): <25% of neurons showing pyknotic nuclei (condensed, hyperchromatic, shrunken) or cytoplasmic shrinkage. Moderate (++): 25–50% of neurons affected by pyknotic or degenerative changes. Severe (+++): >50% of neurons displaying severe pyknosis, cytoplasmic vacuolization, or loss of normal cellular architecture. These criteria were adapted from established histopathological scoring systems for experimental models of diabetic neuropathy and neurotoxicity [26, 27]. Quantitative analysis was performed using ImageJ software (ImageJ bundled with 64-bit Java 1.8.0_112, Wayne Rasband, National Institute of Health, Bethesda, MD, USA), all assessments being performed by a histopathologist who was masked to group allocation.

In situ hybridization

The staining procedure utilized oligonucleotides rno-miR-124-5p (5Dig/ATCAAGGTCCGCTGTGAACACG) and rno-miR-144-5p (5Dig/ACTTACAGTATATGATGATATCC). Paraffin-embedded tissue was sectioned at 4 µm thickness and placed onto poly-L-lysine-coated glass slides. While these slides provided adequate tissue adhesion under our experimental conditions, we note that positively charged glass slides (e.g., SuperFrost Plus) may be preferable in future studies to further minimize tissue detachment during enzymatic digestion and elevated temperature incubations. The mounted sections underwent thermal conditioning at 57 °C for 60 min before deparaffinization via sequential xylene and graded alcohol baths. After washing with PBS, the sections were treated with Proteinase K at 10 µg/mL in 50 mM Tris-HCl, 5 mM EDTA, pH 8.0 for 10 min at room temperature, which was optimized to achieve sufficient tissue permeabilization while preserving RNA integrity. Prehybridization solution was applied at 50 °C for 3 h, and sections were incubated overnight at 45 °C with digoxigenin-labeled probes at a working concentration of 50 nM in hybridization solution. Following hybridization, slides were washed in 2× SSC for 10 min at room temperature, followed by two washes in 0.5× SSC at 55 °C for 15 min each. A final high-stringency wash was performed in 0.1× SSC at 60 °C for 10 min. Sections were then equilibrated in PBS and subjected to a blocking step. After blocking, the sections were incubated with anti-DIG antibody (1:50 dilution) at room temperature for 4 h, followed by three 10-minute washes with PBS and two 5-minute washes with alkaline phosphatase buffer. Staining was performed using 6.6 µL NBT and 3.3 µL BCIP per 1 mL of AP buffer, resulting in final concentrations of 33 µM NBT and 16.5 µM BCIP, at room temperature. Sections were then washed with distilled water, counterstained, and examined under a microscope.

Control experiments included sections hybridized with a scrambled sequence probe of comparable length and GC content as a negative control, which consistently showed no detectable staining following NBT/BCIP development, indicating that endogenous alkaline phosphatase activity did not contribute to background signal. A probe targeting U6 snRNA was used as a positive control to verify RNA integrity and ISH efficiency; robust and consistent U6 staining was observed in all samples. For quantification, miRNA expressions were analyzed in six randomly selected cortex areas at ×20 magnification using the ImageJ program (ImageJ bundled with 64-bit Java 1.8.0_112, Wayne Rasband, National Institutes of Health, Bethesda, MD, USA).

RNA isolation, cDNA synthesis, and qRT-PCR analysis

The expression levels of miR-124-5p and miR-144-5p in tissue and serum samples were evaluated using real-time polymerase chain reaction (qRT-PCR). For this purpose, RNA isolation, cDNA synthesis, and qRT-PCR procedures were carried out according to the following protocols.

RNA isolation from tissue and serum samples stored at -80 °C was performed using the EcoPURE Total RNA Kit (Ecotech Biotechnology, Erzurum, Türkiye) and TRUEzol LS Reagent (Ecotech Biotechnology, Erzurum, Türkiye), following the manufacturer's protocol. The concentration and purity of the RNA samples were measured using an Epoch Microplate Spectrophotometer (BioTek Instruments,

Winooski, VT, USA) [28]. Due to the limited size of the tissue samples, comparable tissue fragments of similar size were used for RNA isolation rather than weighing each specimen individually. Tissue samples used for RNA isolation and antioxidant enzyme assays were processed using independent tissue portions.

cDNA synthesis was performed using 1000 ng of RNA from tissue samples and 100 ng of RNA from serum samples. The cDNA synthesis was carried out using the 'High Capacity cDNA Reverse Transcription Kit' (Thermo Fisher Scientific, USA) and stem-loop RT primers according to the manufacturer's protocol. For miRNA reverse transcription, miRNA-specific stem-loop RT primers were used to enable the specific reverse transcription of mature miRNAs prior to qRT-PCR analysis. The stem-loop RT primers and corresponding miRNA-specific qPCR primers were designed according to the stem-loop RT-qPCR strategy described by Kramer [29]. Amplification reactions utilized 5x HOT FIREPol® EvaGreen® qPCR Mix following the manufacturer's instructions, with a Rotor-Gene Q Real-Time PCR (Qiagen). For expression analysis in tissue samples, the RNU43 was used as an internal control, while RNU6b (U6) was used as an internal control for serum sample expression analysis. The Ct values of the reference genes were evaluated and showed no significant variation among the experimental groups, indicating stable expression under the experimental conditions. The experiments were performed at least in duplicates. Relative quantification analysis was conducted using the 2^-ΔCt method [29]. The primer sequences used in the study are provided in Table 1.

Table 1 qRT-PCR Primer Sequences

Gene	Primer	Sequence
RNU43	Forward	5'-CAAATGATGAATCCTTTGACGGGC-3'
	Reverse	5'-AGATCAGAACATGACAATCAGCAC-3'
U6	Forward	5'-CGCTTCGGCAGCACATATACT-3'
	Reverse	5'-ACGCTTCACGAATTTGCGTG-3'
rno-miR-124-5p	Stem loop	5'-GTCGTATCCAGTGCAGGGTCCGAGGTATTCGCACTGGATACGACATCAAG-3'
	Forward	5'-CACGCACGTGTTCACAGC-3'
	Reverse	5'-CAGTGCAGGGTCCGAGGTA-3'
rno-miR-144-5p	Stem loop	5'-GTCGTATCCAGTGCAGGGTCCGAGGTATTCGCACTGGATACGACACTTAC-3'
	Forward	5'-CGCGCGCGGATATCATCATA-3'
	Reverse	5'-CAGTGCAGGGTCCGAGGTA-3'

Biochemical examination

Brain specimens designated for biochemical assessment were procured immediately after sacrifice and preserved at -80 °C until the time of analysis. Tissue disruption was carried out under cryogenic conditions using a TissueLyser device (Qiagen, Hilden, Germany), with homogenization performed in PBS at a ratio of 1 mL per 50 mg tissue. The resulting homogenates were clarified by centrifugation. In all homogenates, levels of reduced glutathione (GSH), malondialdehyde (MDA), nitric oxide synthase (NOS), and aldose reductase (AR) were quantified with validated commercial ELISA platforms according to each manufacturer's recommended protocol. Levels of GSH (SunRed, Catalog No: 201-11-5134), MDA (SunRed, Catalog No: 201-11-0157), NOS (SunRed, Catalog No: 201-11-0705), AR (SunRed, Catalog No: 201-11-6135) were reported in mg/L, nmol/mL, ng/mL, and ng/mL, (per gram of wet tissue) respectively.

Immunohistochemical method

Tissue Sect. (5 µm) mounted on poly-L-lysine–coated slides were deparaffinized in xylol, rehydrated through a descending alcohol gradient, rinsed in PBS, and treated with 3% hydrogen peroxide for 10 min to quench endogenous peroxidase activity. To release the antigen in the tissues, they were treated with antigen retrieval solution at 500 W for 2 × 5 min. Following a non-specific protein blocking step and PBS rinse, sections were exposed to anti-caspase-3 primary antibody (1:200 working dilution) at 4 °C for an overnight incubation period. As secondary; Large Volume Detection System: Anti-Polyvalent, HRP (Thermo Fisher, Catalog No: TP-125-HL) was used as recommended by the manufacturer. DAB (3,3'-diaminobenzidine) was used as chromogen. After counterstaining with Mayer's hematoxylin, they were covered with aqueous mounting medium and examined under a light microscope. Immunopositivity intensities in 6 different random cortex areas at ×20 magnification were evaluated in ImageJ software.

Statistical analysis

All statistical computations were executed in SPSS v25.0 (IBM Corp., Armonk, NY) in conjunction with GraphPad Prism 9.0 (San Diego, CA). Distribution normality was confirmed via the Kolmogorov–Smirnov procedure and variance equality by Levene's test prior to parametric analyses. All variables satisfied these distributional prerequisites ($p > 0.05$ for both tests). For biochemical parameters, histopathological scores, immunohistochemical quantification, and in situ hybridization data, inter-group comparisons were

conducted by one-way ANOVA with Tukey's multiple comparison correction. Values are reported as mean ± SD for $n = 10$ per group. For qRT-PCR gene expression data, statistical comparisons between control and treatment groups were performed using Student's t-test. Expression data are presented as mean ± standard error of the mean (SEM). Statistical significance was defined at a threshold of $p < 0.05$. All statistical tests were two-tailed.

Results

Blood glucose levels

Diabetes confirmation was performed 72 h after STZ administration by measuring tail-vein FBG. Animals exhibiting FBG exceeding 250 mg/dL were classified as diabetic and enrolled, whereas those not achieving this glycemic threshold were excluded to guarantee sustained hyperglycemic status. Fasting blood glucose levels were reassessed at the end of the 10-week intervention to monitor both the persistence of diabetes and the effects of the SN treatment. Inclusion criteria were male Sprague Dawley rats aged 7 week with body weight 200 ± 20 g, and confirmed hyperglycemia after STZ injection. Exclusion criteria included rats failing to develop hyperglycemia or exhibiting severe health complications during the study period. STZ injection produced consistent hyperglycemia across both the DM and DM + SN cohorts by 72 h post-administration (265.0 ± 31.12 and 265.0 ± 39.11 mg/dL, respectively) compared to control groups ($p < 0.001$). By week 10, untreated DM animals displayed a progressive glycemic escalation (485.0 ± 40.01 mg/dL), indicating progressive hyperglycemia. Notably, SN-supplemented diabetic rats showed a pronounced attenuation of hyperglycemia (127.0 ± 39.11 mg/dL at week 10; $p < 0.001$ compared to DM group), reflecting considerable hypoglycemic potency of the extract. Control and SN-only groups maintained normoglycemic levels throughout the study period (Table 2).

Mean body weight levels measured at baseline and at week 10 of the intervention were reported in Table 2. There were significant differences in terms of body weight in control, SN, and DM + SN groups in the 10.week compared to baseline levels.

Table 2 Mean fasting blood glucose and body weight levels measured at baseline/72 h and at week 10 of the intervention

Fasting Blood Glucose (mg/dL)			
Groups	72 h	Week 10	p-value*
Control	82.22 ± 16.91[a]	84.02 ± 2.14[a]	0.950
SN	82.00 ± 16.15[b]	80.98 ± 16.16[b]	0.100
DM	265.0 ± 31.12[c]	485.0 ± 40.01[c]	0.850
DM + SN	265.0 ± 39.11[d, e]	127.0 ± 39.11[d, e]	0.185
p-value**	0.000	0.000	
Body Weight (g)			
Groups	Baseline	Week 10	p-value*
Control	208.2 ± 6.0	258.0 ± 3.3[a]	< 0.001
SN	208.3 ± 5.1	257.3 ± 3.6[b]	< 0.001
DM	211.3 ± 5.7	218.2 ± 4.0[c]	0.011
DM + SN	210.4 ± 6.3	237.1 ± 4.4[d, e]	< 0.001
p-value**	0.559	< 0.001	

DM: diabetes group, SN: *sambucus nigra* extract group, DM + SN: diabetes and *sambucus nigra* extract group. *Notes*: *Comparison within groups using paired-samples t-test. **Comparison among groups using One-way ANOVA test. [a, b,c, d,e] Different superscript letters indicate statistically significant differences between groups ($p < 0.05$). Values are expressed as mean ± SD; $N = 10$; $p < 0.05$ was considered statistically significant

Oxidative stress and biochemical parameters

To assess the impact of diabetes on oxidative/nitrosative stress and the protective effects of SN extract, we measured GSH, MDA, NOS, and AR levels in both brain tissue (expressed per gram of wet tissue) and serum (Fig. 1). Oxidative stress markers (GSH, MDA), nitrosative stress indicator (NOS), and polyol pathway enzyme (AR) levels in brain tissue and serum are presented in Fig. 1. All one-way ANOVA tests (AR, MDA, GSH, NOS both in brain tissues (expressed per gram of wet tissue) and serum samples) resulted significant p values ($p < 0.05$). Post-hoc Tukey test demonstrated statistically significant differences across all parameters in both brain tissue (Fig. 1A) and serum (Fig. 1B) among experimental groups. In diabetic rats, MDA levels were significantly elevated while GSH levels were markedly decreased, indicating severe oxidative stress. SN treatment effectively reversed these alterations, reducing MDA and restoring GSH to near-control levels. Similarly, NOS activity and AR levels, which were altered in the diabetic condition, showed significant improvement with SN administration ($p < 0.01$). Figure 1. Levels of GSH, MDA, NOS, and AR expression were measured in brain tissue samples through biochemical analysis. Data are presented as mean ± SD ($n = 10$ per group). Statistical analysis was performed using one-way ANOVA followed by Tukey's post hoc test. *$p < 0.05$, **$p < 0.01$, ***$p < 0.001$.

qRT-PCR results

To probe the molecular underpinnings of SN-mediated neural protection, we profiled the abundance of two diabetes-linked miRNAs (miR-124-5p and miR-144-5p) across brain parenchyma and circulating serum fractions (Fig. 2). The analysis of miR-124-5p and miR-144-5p in barian tissue samples of differrent groups, we found that the expression level of miR-124-5p significantly decreased in the DM group compared to the Control group (Fig. 2A).

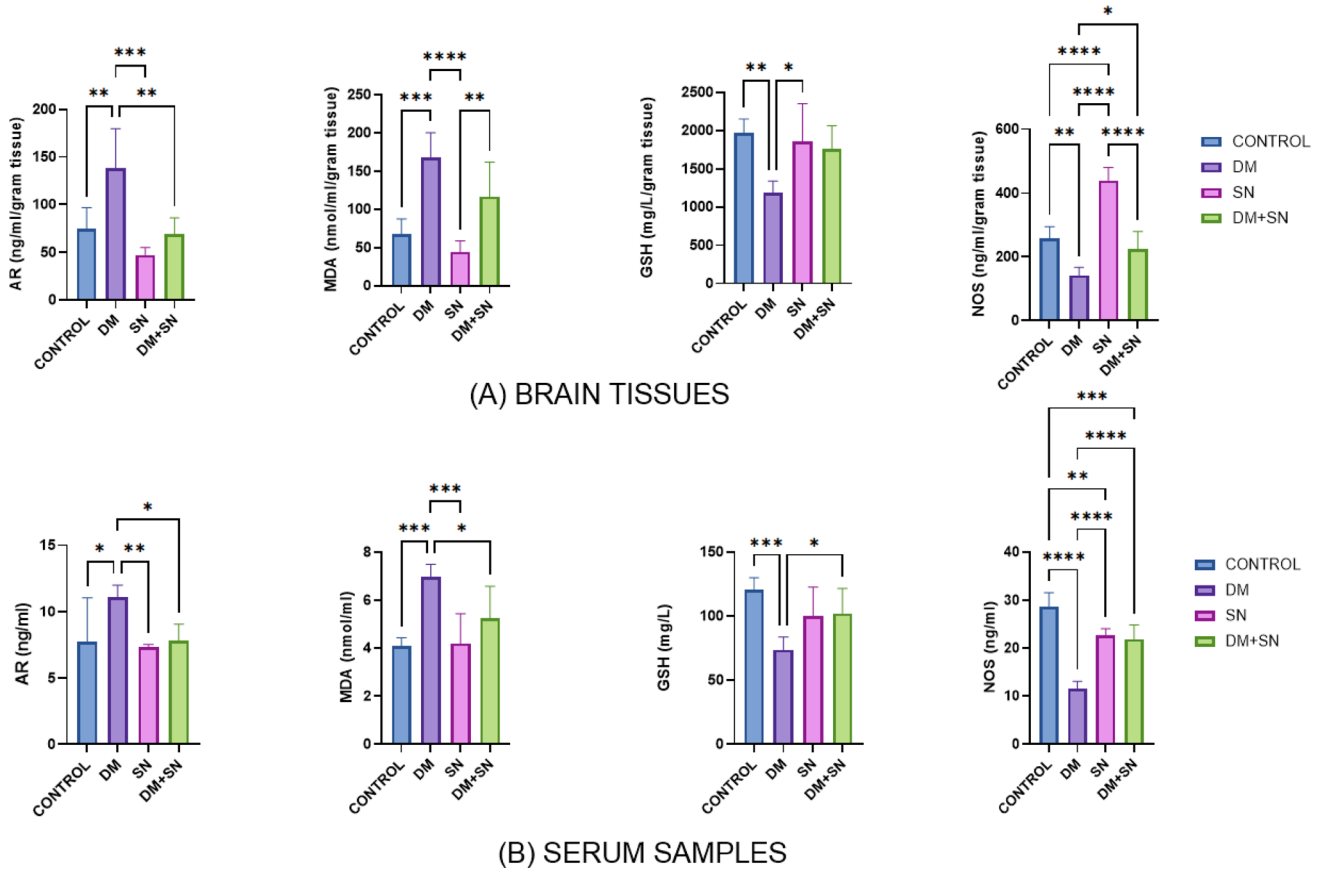


Fig. 1 Levels of GSH, MDA, NOS, and AR expression were measured in (**A**) brain tissues (expressed per gram of wet tissue) and (**B**) serum samples through biochemical analysis. Data are presented as mean ± SD (n = 10 per group). Statistical analysis was performed using one-way ANOVA followed by Tukey's post hoc test. *$p < 0.05$, **$p < 0.01$, ***$p < 0.001$, ****$p < 0.001$

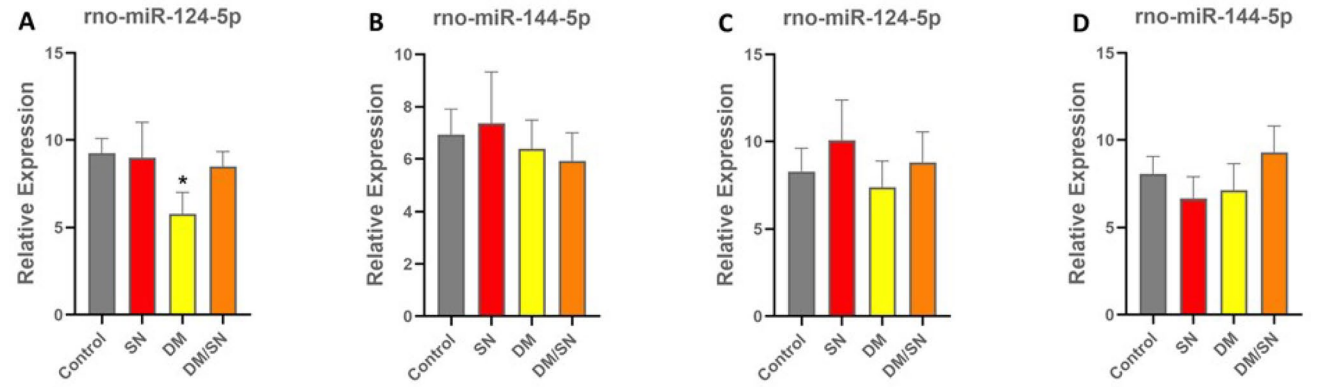


Fig. 2 Expression of rno-miR-124-5p (**A**) and rno-miR-144-5p (**B**) in brain tissue samples. Expression of rno-miR-124-5p (**C**) and rno-miR-144-5p (**D**) in serum samples. Data are presented as mean ± SEM (n = 10 per group). Statistical analysis was performed using one-way ANOVA followed by Tukey's post hoc test. *$p < 0.05$

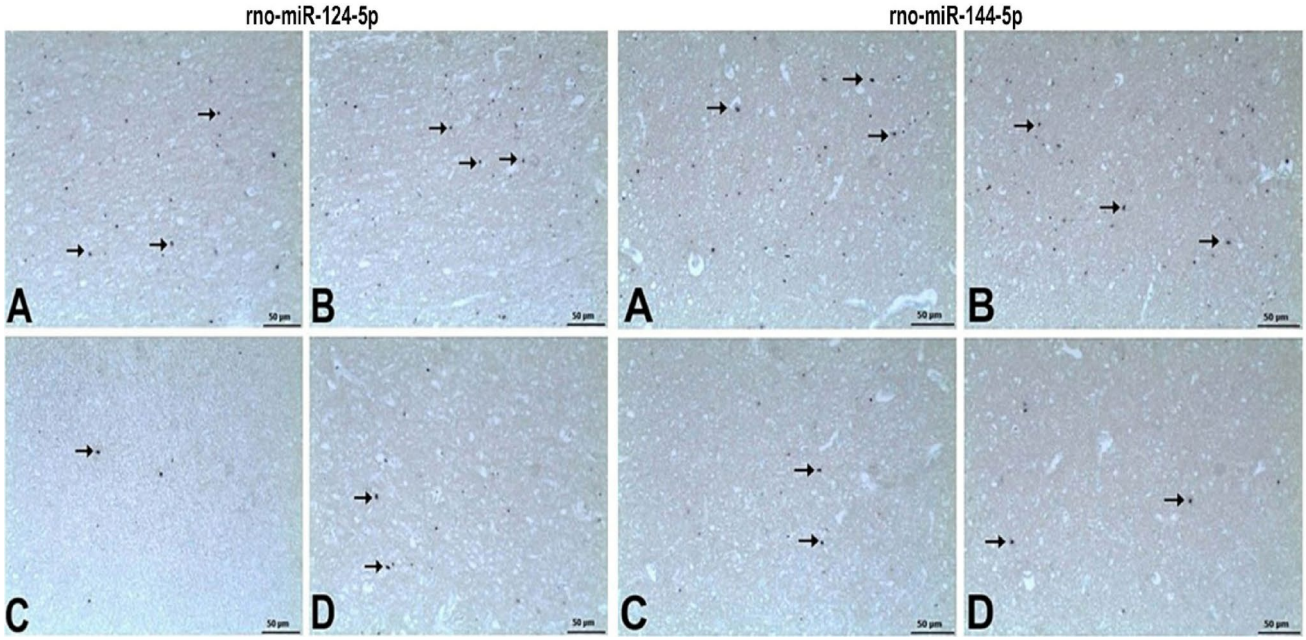


Fig. 3 rno-miR-124-5p expression. (**A**) Control group, (**B**) SN group; severe expression, (**C**) DM group; mild expression, (**D**) DM + SN group; moderate expression (→), rno-miR-144-5p expression. A-Control group, B- SN group; severe expression, C- DM group; moderate expression, D- DM + SN group; moderate expression, (→). Scale bar: 50 µm; magnification: ×20. IHC

Table 3 Statistical analysis of the expression levels of rno-miR-124-5p and rno-miR-144-5p

Groups	rno-miR-124-5p	rno-miR-144-5p
Control	14.51 ± 4.31^{a}	17.32 ± 5.90^{a}
SN	16.09 ± 5.83^{a}	15.94 ± 6.24^{a}
DM	4.27 ± 2.18^{b}	9.41 ± 4.85^{b}
DM + SN	9.04 ± 4.16^{c}	8.17 ± 5.01^{b}

DM: diabetes group, SN: sambucus nigra extract group, DM + SN: diabetes and sambucus nigra extract group. [a, b,c] The difference between groups in the same column ($p < 0.05$)

Additionally, SN-treated diabetic animals displayed a recovery of miR-124-5p levels approaching those observed in the control cohort (Fig. 2A). Furthermore, miR-144-5p abundance in cerebral tissue did not differ significantly across groups (Fig. 2B). Assessment of circulating miRNA profiles revealed that neither miR-124-5p nor miR-144-5p exhibited inter-group variation at the serum level (Fig. 2C-D).

In situ hybridization results

To spatially visualize miRNA expression patterns in brain tissue and validate qRT-PCR findings, in situ hybridization was performed using probes specific for rno-miR-124-5p and rno-miR-144-5p (Figs. 3; Table 3). As shown in Table 3, statistically significant differences were detected among groups in the in situ hybridization staining with rno-miR-124-5p and rno-miR-144-5p oligonucleotides ($p < 0.05$).

In the control and SN groups, the expression levels of rno-miR-124-5p and rno-miR-144-5p were at severe levels. In the DM group, the expression of rno-miR-124-5p was at a mild level, while the expression of rno-miR-144-5p was at a moderate level. In the DM + SN group, both rno-miR-124-5p and rno-miR-144-5p were expressed at a moderate level (Fig. 3).

Immunohistochemical results

To evaluate apoptotic pathway activation in neuronal tissues, we assessed caspase-3 expression, a key executioner enzyme in programmed cell death (Fig. 4; Table 4). Statistically significant differences were detected among groups in the caspase-3 expression evaluation (Table 4).

No significant caspase-3 immunopositivity was detected in the Control and DM group. In the other treatment groups, caspase-3 immunopositivity was found to be severe in the DM group and mild in the DM + SN group (Fig. 4).

Histopathological results

To determine the ultimate morphological consequences of diabetes-induced oxidative stress, miRNA dysregulation, and apoptotic activation, histopathological examination of neuronal integrity was performed (Fig. 5; Table 5). Statistically significant differences were detected among groups in the histopathological evaluation (Table 5).

Cortical neurons in both Control and SN-only animals exhibited intact cytoarchitecture. By contrast, diabetic groups (DM and DM + SN) displayed graded neuronal

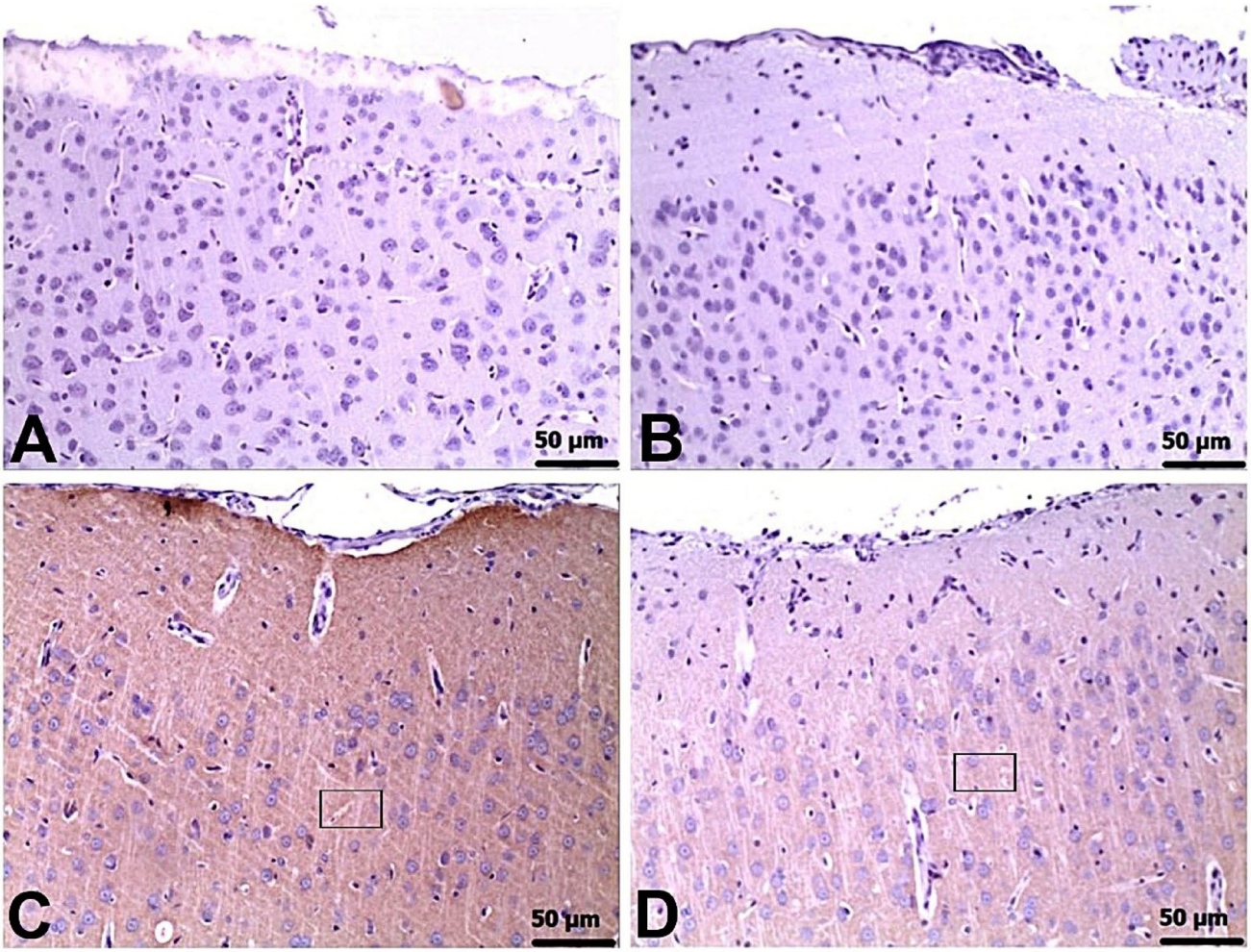


Fig. 4 Immunohistochemical expression of caspase-3 in rat cerebral cortex. **A**- Control group, **B**- SN group; immun negative, **C**- DM group; severe immunpositivity, **D**- DM + SN group; mild immunpositivity, (→). Scale bar: 50 µm; magnification: ×20. IHC

Table 4 Caspase-3 expressions in neurons

Groups	Cortex
Control	4.09 ± 2.18^{a}
SN	5.34 ± 3.29^{a}
DM	78.61 ± 13.46^{b}
DM + SN	27.46 ± 6.39^{c}

DM: diabetes group, SN: sambucus nigra extract group, DM + SN: diabetes and sambucus nigra extract group. Data are presented as mean ± SD ($n = 10$/group). [a, b,c] The difference between groups in the same column ($p < 0.05$)

pathology: the DM group showed pronounced pyknosis and cellular degeneration, whereas the DM + SN group exhibited only mild morphological alterations. Affected neurons were characterized microscopically by nuclear condensation and perikaryal shrinkage (Fig. 5).

Discussion

The present investigation examined the antioxidant and neural-protective capacity of black elderberry (*Sambucus nigra*, SN) extract were investigated in experimentally induced T2DM rats. This study is unique in evaluating the protective effects of SN extract on both brain and serum in an experimental T2DM model. Considering the effects of oxidative stress and sorbitol accumulation in tissues in the pathogenesis of diabetic neuropathy, investigating these effects in both serum and brain tissue is valuable. In addition to histopathological evaluation, molecular and biochemical analyses were conducted to strengthen the results.

Chronic hyperglycemia in T2DM triggers mitochondrial dysfunction and excessive production of reactive oxygen species, leading to oxidative stress that plays a central role in the development of diabetic complications [30]. Our biochemical analyses revealed marked oxidative imbalance in diabetic rats, evidenced by elevated MDA levels and

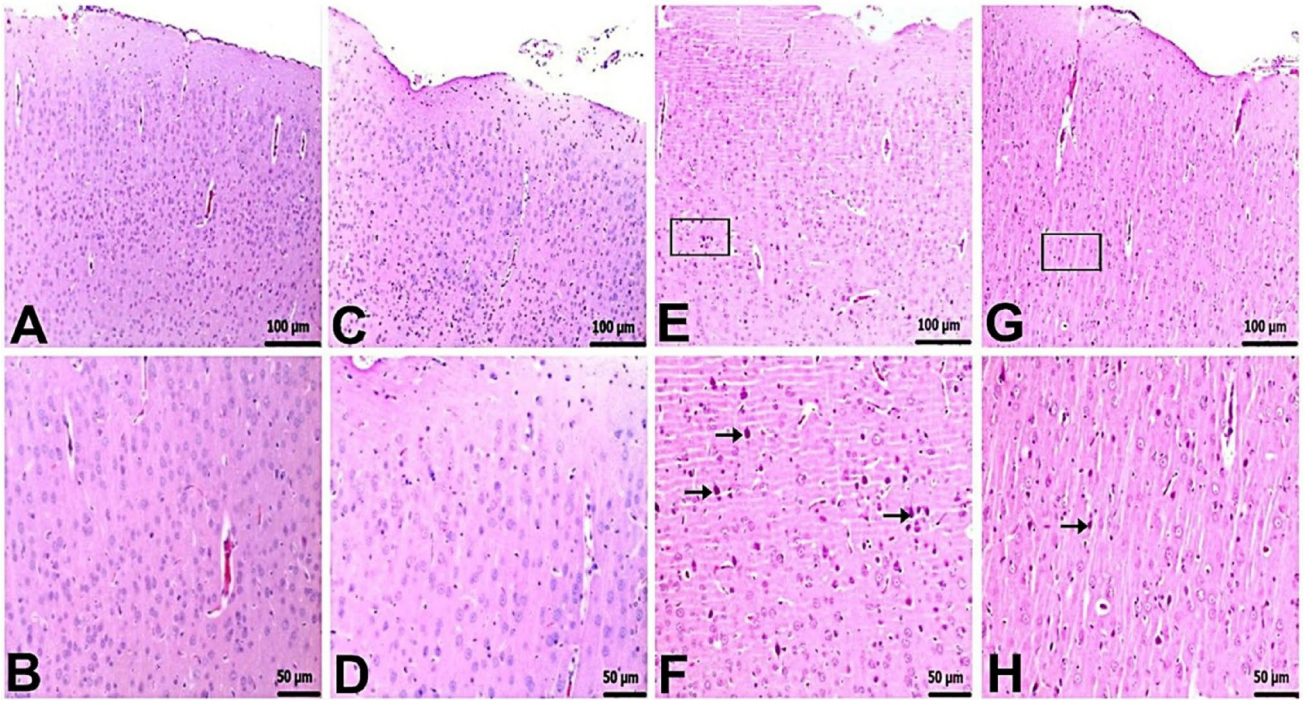


Fig. 5 Histological changes in the rat brain cortex. **A-B** Control group, **C-D** SN group; normal histological appearance, **E-F** DM group; severe pyknosis and degeneration in neurons (□, →), G-H DM + SN group; mild pyknosis and degeneration in neurons (□, →). Scale bar: 100 µm, 50 µm; magnification: ×20. H&E

Table 5 Pyknotic and degenerative changes in neurons

Groups	Cortex
Control	2.26 ± 1.84^{a}
SN	3.15 ± 1.74^{a}
DM	15.84 ± 6.18^{b}
DM + SN	6.71 ± 3.69^{c}

DM: diabetes group, SN: sambucus nigra extract group, DM + SN: diabetes and sambucus nigra extract group. Data are presented as mean ± SD ($n = 10$/group). [a, b,c] The difference between groups in the same column ($p < 0.05$)

depleted GSH levels. SN extract effectively reversed these alterations, restoring both parameters to near-control levels ($p < 0.01$). This redox-modulatory effect carries substantial mechanistic weight, as oxidative burden constitutes the proximal instigator of several deleterious downstream cascades: suppression of neuroprotective miRNA pools, compromise of mitochondrial bioenergetics, and engagement of programmed cell death signaling [31]. By neutralizing reactive oxygen species through its polyphenolic compounds, SN extract interrupts this initiating pathological mechanism. These findings align with studies demonstrating antioxidant effects of polyphenol-rich extracts in diabetic models [9, 32]. In this context, a study conducted on mice found that SN extract has a reducing effect on oxidative DNA damage [33]. This result suggests that SN extract has antioxidant properties and may protect cells from the harmful effects of free radicals. Our data indicated that diabetic conditions elevated MDA—a terminal byproduct of membrane lipid peroxidation widely employed as an oxidative damage index—whereas SN supplementation attenuated these elevations. Conversely, the endogenous antioxidant defenses reflected by GSH content and NOS activity were depleted under hyperglycemic stress but substantially recovered upon SN administration. In an experimental study investigating the efficacy of SN extract in diabetes within a gold nanoparticulate formulation, SN extract increased the GSH/GSSG ratio in muscle tissue and circulation, and decreased MDA levels in rats with diabetes induced by streptozotocin. Researchers have suggested that gold nanoparticulate with SN extract offers a great potential as an adjuvant for diabetes treatment due to its ability to increase antioxidant defense and reduce inflammation in liver tissue [34].

Furthermore, a notable observation in our study was that SN extract's regulatory effect on aldose reductase activity, a critical enzyme in the polyol pathway. Under hyperglycemic conditions, increased aldose reductase activity leads to excessive sorbitol accumulation in neural tissues, triggering osmotic stress and contributing to diabetic neuropathy [35]. Our results demonstrated that SN extract significantly attenuated the diabetes-induced elevation of aldose reductase activity in brain tissue. The modulation of aldose reductase by SN extract likely occurs through the direct interaction of its polyphenolic compounds with the enzyme's active site, similar to the mechanism reported for quercetin derivatives

[36]. This regulation of the polyol pathway not only protects against neuronal damage but may also help prevent other diabetes-related microvascular complications where aldose reductase plays a pathogenic role [37].

From a molecular signaling perspective, the neuroprotective mechanism of SN extract appears to involve several interconnected pathways beyond direct antioxidant scavenging. Recent evidence has demonstrated that SN extract activates the nuclear factor erythroid 2-related factor 2/heme oxygenase-1 (Nrf2/HO-1) signaling cascade, a master regulator of the cellular antioxidant defense system [38]. Activation of Nrf2 promotes the transcription of cytoprotective genes including HO-1, NAD(P)H quinone dehydrogenase 1 (NQO1), and glutathione S-transferase, collectively enhancing the cell's capacity to neutralize reactive oxygen species and electrophilic stress. Concurrently, SN bioactive compounds particularly quercetin, rutin, and cyanidin-3-glucoside have been shown to suppress the nuclear factor-kappa B (NF-κB) inflammatory signaling pathway, thereby reducing the production of pro-inflammatory cytokines such as tumor necrosis factor-alpha (TNF-α), interleukin-1β (IL-1β), and interleukin-6 (IL-6) [39, 40]. The crosstalk between Nrf2 activation and NF-κB suppression is particularly relevant in diabetic neuropathy, as chronic hyperglycemia-induced NF-κB activation drives neuroinflammation, which in turn exacerbates oxidative damage and neuronal apoptosis. Furthermore [41], demonstrated that aqueous SN extract promotes neuroprotection partly through inhibition of mammalian target of rapamycin complex 1 (mTORC1) and recovery of autophagy in neuronal cell models, suggesting that SN may facilitate the clearance of damaged cellular components and misfolded proteins that accumulate under diabetic conditions. Additionally, narcissoside, a flavonoid glycoside isolated from SN flowers, has been shown to exert neuroprotective effects through enhancement of the miR200a/Nrf2/GSH axis and modulation of ERK/Akt signaling while inhibiting JNK and p38 MAPK phosphorylation in neurotoxicity models [42]. These converging molecular pathways collectively explain the observed reduction in oxidative stress markers, attenuation of caspase-3-mediated apoptosis, and preservation of miR-124-5p expression in SN-treated diabetic rats in the present study.

The molecular mechanisms underlying SN's neuroprotective effects were further evidenced by our miRNA expression analyses. We observed that miR-124-5p expression significantly decreased in diabetic rat brain tissue and was restored to near-control levels following SN treatment. This finding requires careful interpretation within the context of tissue-specific miRNA regulation. miR-124, the most abundant miRNA in the brain, exhibits paradoxical expression patterns across different tissues in diabetes. While [43] and [44] report elevated miR-124 in serum and pancreatic tissues of diabetic patients where it negatively regulates insulin secretion, our observation of decreased brain miR-124 aligns with findings in other diabetic tissues showing miR-124 suppression under oxidative stress conditions. Liang et al. [45] demonstrated that miR-124-3p expression decreases in diabetic kidney disease, where it regulates mitochondrial function through the FOXQ1/Sirt4 pathway. Similarly, in another study using an in vitro diabetic retinopathy model, it was shown that miR-124 suppresses the function of G3BP2, which regulates the p38MAPK signaling pathway, thereby regulating the impaired functions of human retinal microvascular endothelial cells induced by high glucose, suggesting that miR-124 could be used as a potential biomarker in diabetic retinopathy treatment [46]. These studies suggest that miR-124 acts as a protective factor in multiple tissues, and its suppression under diabetic conditions contributes to cellular dysfunction. The restoration of miR-124 by SN treatment likely reflects the extract's ability to reduce oxidative stress and preserve protective signaling pathways, thereby maintaining cellular integrity and mitochondrial function in brain tissue. Yu et al. [47] showed that miR-144 inhibition reduces cardiac apoptosis in diabetic mice, while Ekta et al. [48] reported its upregulation in diabetic liver damage. This tissue-specific pattern suggests that miR-144 dysregulation primarily affects metabolic and cardiovascular systems rather than brain tissue in our experimental model. The modest changes observed by in situ hybridization, which were not confirmed by qRT-PCR, may reflect regional or cellular heterogeneity within brain structures that is masked when analyzing whole-tissue homogenates. Our findings demonstrated that SN extract modulates diabetes-associated miRNA dysregulation in a tissue-appropriate manner, restoring miR-124-mediated neuroprotective signaling pathways without affecting miR-144 expression in brain tissue. This selective miRNA modulation, combined with direct antioxidant effects and reduced caspase-3 activation, contributes to the observed neuronal protection.

Programmed apoptotic cell death, governed by tightly coordinated gene programs and frequently implicated in neurodegenerative pathology, represents a pivotal route through which hyperglycemia inflicts irreversible neuronal loss [49]. The executioner protease caspase-3 occupies a central position in this apoptotic cascade and constitutes a decisive effector of neuronal demise within the central nervous system [50]. Our immunohistochemical findings demonstrated significantly increased caspase-3 expression in the cerebral cortex of diabetic rats, indicating enhanced neuronal apoptosis. Treatment with SN extract markedly attenuated this diabetes-induced apoptotic response, as evidenced by reduced caspase-3 immunoreactivity. This neuroprotective effect aligns with recent study demonstrating

that anthocyanin-rich extracts prevent neuronal apoptosis in diabetic models by modulating the Bcl-2/Bax pathway and suppressing caspase activation [51]. The mechanism underlying SN's anti-apoptotic effect appears multifactorial: our findings demonstrate that SN extract reduces oxidative stress (decreased MDA, increased GSH and NOS), which prevents mitochondrial dysfunction and subsequent caspase-3 activation. Additionally, the restoration of miR-124-5p expression in SN-treated diabetic rats may contribute to anti-apoptotic signaling, as this miRNA regulates multiple pathways involved in neuronal survival and glucose metabolism [52].

The histopathological evidence of reduced neuronal pyknosis and degeneration in SN-treated diabetic brains provides critical validation that molecular and biochemical improvements translate to preserved tissue integrity. This concordance between markers (restored miR-124, reduced caspase-3), biochemical parameters (normalized oxidative stress, decreased aldose reductase), and morphology demonstrates an integrated protective mechanism rather than isolated effects.

Several limitations should be acknowledged. First, the single-dose design without dose-response evaluation limits determination of optimal therapeutic ranges and prevents comparison with standard pharmacological agents. Second, while caspase-3 immunoreactivity provided evidence of apoptosis, additional markers such as Bax, Bcl-2, and TUNEL assay would offer more comprehensive characterization of apoptotic pathway modulation. Third, although we have discussed the possible involvement of Nrf2/HO-1, NF-κB, and mTORC1/autophagy pathways based on published evidence with SN extract, direct measurement of these signaling molecules was not performed in the present study and warrants investigation in future research. Fourth, as we could not determine the total protein concentration, we reported the results on a per gram of wet tissue weight basis, not on milligrams of protein per wet tissue. Future studies should incorporate dose-response designs with pharmacological controls, comprehensive apoptotic and antioxidant enzyme profiling, detailed signaling pathway analyses (including Nrf2, NF-κB, and PI3K/Akt), and mechanistic investigations to establish SN extract's clinical translation potential for diabetic neuropathy management.

Conclusion

Taken together, our findings establish that SN extract confers pronounced antidiabetic and neuroprotective benefits in a streptozotocin-induced T2DM rat model, with results consistent with the literature highlighting its antioxidant properties. The extract modulated miR-124-5p and miR-144-5p expression, suppressed neuronal apoptosis as evidenced by reduced caspase-3 immunoreactivity, and improved oxidative stress markers by decreasing MDA levels while increasing GSH and NOS. These molecular and biochemical improvements were supported by histopathological evidence showing reduced neuronal degeneration. These results position SN extract as a candidate adjunctive intervention for T2DM management and the prevention of associated neurological sequelae. Further research should investigate the clinical relevance of these findings and the potential for integrating SN extract into therapeutic regimens for diabetic patients, with a focus on understanding the precise molecular mechanisms involved. Future studies should also explore apoptotic signaling pathways in greater detail, including the evaluation of gene expression and additional molecular markers related to apoptosis.

Supplementary Information The online version contains supplementary material available at https://doi.org/10.1007/s11033-026-11899-4.

Acknowledgements Research reported in this publication was supported by Atatürk University Scientific Research Projects Coordination Unit under award number TKP-2023-11848.

Author contributions AG, OFK, NKB, HA, MO, EKS, FS, and HU designed experimental setup, collected samples and carried out experiments. OFK, FS, and MO were involved in molecular investigation. All the authors contributed to the writing and editing, and they read and approved the manuscript.

Data availability The datasets used and/or analysed during the current study available from the corresponding author on reasonable request.

Declarations

Competing interests The authors declare no competing interests.

References

1. Magliano DJ, Boyko EJ, Atlas D (2025) 3. The global picture of diabetes, Diabetes Atlas [Internet]. 11th edition, International Diabetes Federation
2. Nuhoglu I, Deger O, Topbaş M, Erem C (2022) The prevalence of diabetes and associated risk factors among adult population in a Turkish population (Trabzon city). Prim Care Diabetes 16:549–554
3. Satman I, Omer B, Tutuncu Y, Kalaca S, Gedik S, Dinccag N, Karsidag K, Genc S, Telci A, Canbaz B (2013) Twelve-year trends in the prevalence and risk factors of diabetes and prediabetes in Turkish adults. Eur J Epidemiol 28:169–180
4. Aktas G, Atak Tel BM, Tel R, Balci B (2023) Treatment of type 2 diabetes patients with heart conditions. Expert Rev Endocrinol Metabolism 18:255–265
5. Abbatecola AM, Arosio B, Cerasuolo M, Auriemma MC, Di Meo I, Langiano E, Rizzo MR (2024) Common neurodegenerative pathways in brain aging, cognitive decline, type 2 diabetes & metabolic syndrome. J Gerontol Geriatr 72:43–49

6. Han D, Dong X, Zheng D, Nao J (2020) MiR-124 and the underlying therapeutic promise of neurodegenerative disorders. Front Pharmacol 10:1555
7. Lin W, Tang Y, Zhao Y, Zhao J, Zhang L, Wei W, Chen J (2020) MiR-144-3p targets FoxO1 to reduce its regulation of adiponectin and promote adipogenesis. Front Genet 11:603144
8. Sarasso E, Agosta F, Piramide N, Filippi M (2021) Progression of grey and white matter brain damage in Parkinson's disease: a critical review of structural MRI literature. J Neurol 268:3144–3179
9. Infante-Garcia C, Garcia-Alloza M (2019) Review of the effect of natural compounds and extracts on neurodegeneration in animal models of diabetes mellitus. Int J Mol Sci 20:2533
10. Liu D, He X-Q, Wu D-T, Li H-B, Feng Y-B, Zou L, Gan R-Y (2022) Elderberry (Sambucus nigra L.): Bioactive compounds, health functions, and applications. J Agric Food Chem 70:4202–4220
11. Yalcin O, Bassil NV, Kafkas NE (2022) Wild edible small fruits in Turkey and their fruit characteristics, Proceedings of the Latvian Academy of Sciences, De Gruyter Poland, pp. 417–423
12. Domínguez R, Zhang L, Rocchetti G, Lucini L, Pateiro M, Munekata PE, Lorenzo JM (2020) Elderberry (Sambucus nigra L.) as potential source of antioxidants. Characterization, optimization of extraction parameters and bioactive properties. Food Chem 330:127266
13. Szot I, Łysiak GP, Sosnowska B, Chojdak-Łukasiewicz J (2024) Health-promoting properties of anthocyanins from cornelian cherry (Cornus mas L.) fruits. Molecules 29:449
14. Boscaro V, Rivoira M, Sgorbini B, Bordano V, Dadone F, Gallicchio M, Pons A, Benetti E, Rosa AC (2022) Evidence-based anti-diabetic properties of plant from the Occitan Valleys of the Piedmont Alps. Pharmaceutics 14:2371
15. Osman AG, Avula B, Katragunta K, Ali Z, Chittiboyina AG, Khan IA (2023) Elderberry extracts: Characterization of the polyphenolic chemical composition, quality consistency, safety, adulteration, and attenuation of oxidative stress-and inflammation-induced health disorders. Molecules 28:3148
16. Wilczynska A, Bushell M (2015) The complexity of miRNA-mediated repression. Cell Death Differ 22:22–33
17. Alamro H, Bajic V, Macvanin MT, Isenovic ER, Gojobori T, Essack M, Gao X (2023) Type 2 Diabetes Mellitus and its comorbidity, Alzheimer's disease: Identifying critical microRNA using machine learning. Front Endocrinol 13:1084656
18. Zhang W, Dong X, Huang R (2023) Antiparkinsonian effects of polyphenols: a narrative review with a focus on the modulation of the gut-brain axis. Pharmacol Res 193:106787
19. Vasu S, Kumano K, Darden CM, Rahman I, Lawrence MC, Naziruddin B (2019) MicroRNA signatures as future biomarkers for diagnosis of diabetes states. Cells 8:1533
20. Zhang X, Shao S, Zhao X, Zhang M, Wang J (2022) Micro-RNA-124-5p promotes insulin producing cell differentiation through regulating transcriptional factor NKX6. 1. Biochem Biophys Rep 30:101273
21. De Sousa RAL, Improta-Caria AC (2022) Regulation of microRNAs in Alzheimer´ s disease, type 2 diabetes, and aerobic exercise training. Metab Brain Dis 37:559–580
22. Peña-Bautista C, Tarazona-Sánchez A, Braza-Boils A, Balaguer A, Ferré-González L, Cañada-Martínez AJ, Baquero M (2022) Cháfer-Pericás, Plasma microRNAs as potential biomarkers in early Alzheimer disease expression. Sci Rep 12:15589
23. Gündoğdu H, Uluman E, Yıldız SE, Kılıçle PA, Gezer A, Sarı EK (2023) Therapeutic effect of pomegranate peel extract on heme oxygen-free 1 (HO-1) and angiotensin-converting enzyme-2 (ACE-2) in the kidney tissue of mice treated with mitomycin: Effect of pomegranate peel on HO-1 and ACE-2 in the kidney tissue of mice treated with mitomycin. Rats 1:27–34
24. Badescu M, Badulescu O, Badescu L, Ciocoiu M (2015) Effects of Sambucus nigra and Aronia melanocarpa extracts on immune system disorders within diabetes mellitus. Pharm Biol 53:533–539
25. Sharma M, Chan HK, Lavilla CA Jr, Uy MM, Froemming GRA, Okechukwu PN (2023) Induction of a single dose of streptozotocin (50 mg) in rat model causes insulin resistance with type 2 diabetes mellitus. Fundam Clin Pharmacol 37:769–778
26. Dundar B, Agac B, Alzayadneh E, Tashjian R, Conway KS (2024) The presence of shrunken neurons with pyknotic nuclei in the dentate nucleus is a common postmortem change associated with autolysis of the cerebellar granular cell layer. Free Neuropathology 5:13
27. Gezer A, Sarı EK, Gelen V, Yıldız SE, Özkaraca M, Bedir G, Çalık F, Eliş İ (2024) Exploring the neuroprotective effects of black garlic ethanol extract on acrylamide-induced brain damage through apoptotic and neurodegenerative pathways. Ankara Üniversitesi Veteriner Fakültesi Dergisi 71(4):395–406
28. Sanli F, Tatar A, Gundogdu B, Karatas OF (2024) IP3R1 dysregulation via mir-200c-3p/SSFA2 axis contributes to taxol resistance in head and neck cancer. Eur J Pharmacol 973:176592
29. Livak KJ, Schmittgen TD (2001) Analysis of relative gene expression data using real-time quantitative PCR and the $2-\Delta\Delta CT$ method. Methods 25:402–408
30. Rochette L, Zeller M, Cottin Y, Vergely C (2014) Diabetes, oxidative stress and therapeutic strategies. Biochim et Biophys Acta (BBA)-General Subj 1840(9):2709–2729
31. Konovalova J, Gerasymchuk D, Parkkinen I, Chmielarz P, Domanskyi A (2019) Interplay between MicroRNAs and oxidative stress in neurodegenerative diseases. Int J Mol Sci 20:6055
32. Gezer A, Özkaraca M, Üstündağ H, Soydan M, Alkanoğlu Ö, Bedir G (2024) Docosahexaenoic acid eliminates endoplasmic reticulum stress and inflammatory pathways in diabetic rat keratopathy. Int Immunopharmacol 140:112871
33. Azevedo T, Ferreira T, Ferreira J, Teixeira F, Ferreira D, Silva-Reis R, Neuparth MJ, Pires MJ, Pinto MdL (2022) Gil da Costa, Supplementation of an anthocyanin-rich elderberry (Sambucus nigra L.) extract in FVB/n mice: A healthier alternative to synthetic colorants. Appl Sci 12:11928
34. Opris R, Tatomir C, Olteanu D, Moldovan R, Moldovan B, David L, Nagy A, Decea N, Kiss ML, Filip GA (2017) The effect of Sambucus nigra L. extract and phytosinthesized gold nanoparticles on diabetic rats. Colloids Surf B 150:192–200
35. Thakur S, Gupta SK, Ali V, Singh P, Verma M (2021) Aldose Reductase: A cause and a potential target for the treatment of diabetic complications. Arch Pharm Res 44:655–667
36. Alam MM, Meerza D, Naseem I (2014) Protective effect of quercetin on hyperglycemia, oxidative stress and DNA damage in alloxan induced type 2 diabetic mice. Life Sci 109(1):8–14
37. Gupta JK (2024) The role of aldose reductase in polyol pathway: An emerging pharmacological target in diabetic complications and associated morbidities. Curr Pharm Biotechnol 25:1073–1081
38. Hahn D, Shin SH, Bae J-S (2020) Natural antioxidant and anti-inflammatory compounds in foodstuff or medicinal herbs inducing heme oxygenase-1 expression. Antioxidants 9:1191
39. Lin P, Hwang E, Ngo HT, Seo SA, Yi T-H (2019) Sambucus nigra L. ameliorates UVB-induced photoaging and inflammatory response in human skin keratinocytes. Cytotechnology 71:1003–1017
40. Tohamy AF, Hassan MH, Prince AM, Nashed MS, Hassanen EI, Soliman MM (2025) Sambucus nigra alleviates fenpropathrin-induced hepatorenal toxicity in rats via modulation of NF-κB/TNF-α axis. Sci Rep 15:28741
41. Palomino O, García-Aguilar A, González A, Guillén C, Benito M, Goya L (2021) Biological actions and molecular mechanisms of

Sambucus nigra L. in neurodegeneration: A cell culture approach. Molecules 26:4829
42. Fu R-H, Tsai C-W, Liu S-P, Chiu S-C, Chen Y-C, Chiang Y-T, Kuo Y-H, Shyu W-C, Lin S-Z (2022) Neuroprotective capability of narcissoside in 6-OHDA-exposed Parkinson's disease models through enhancing the MiR200a/Nrf-2/GSH axis and mediating MAPK/Akt associated signaling pathway. Antioxidants 11:2089
43. Kong L, Zhu J, Han W, Jiang X, Xu M, Zhao Y, Dong Q, Pang Z, Guan Q, Gao L (2011) Significance of serum microRNAs in pre-diabetes and newly diagnosed type 2 diabetes: a clinical study. Acta Diabetol 48:61–69
44. Sebastiani G, Po A, Miele E, Ventriglia G, Ceccarelli E, Bugliani M, Marselli L, Marchetti P, Gulino A, Ferretti E (2015) MicroRNA-124a is hyperexpressed in type 2 diabetic human pancreatic islets and negatively regulates insulin secretion. Acta Diabetol 52:523–530
45. Liang L, Wo C, Yuan Y, Cao H, Tan W, Zhou X, Wang D, Chen R, Shi M, Zhang F (2023) miR-124-3p improves mitochondrial function of renal tubular epithelial cells in db/db mice. FASEB J 37:e22794
46. Zhao H, He Y (2021) MiR-124-3p suppresses the dysfunction of high glucose-stimulated endothelial cells by targeting G3BP2. Front Genet 12:723625
47. Yu M, Liu Y, Zhang B, Shi Y, Cui L, Zhao X (2015) Inhibiting microRNA-144 abates oxidative stress and reduces apoptosis in hearts of streptozotocin-induced diabetic mice. Cardiovasc Pathol 24:375–381
48. Ekta M, Gupta A, Kaur TG, Singh O, Bedi (2020) Pathobiological and molecular connections involved in the high fructose and high fat diet induced diabetes associated nonalcoholic fatty liver disease. Inflamm Res 69:851–867
49. Li Z-G, Zhang W, Grunberger G, Sima AA (2002) Hippocampal neuronal apoptosis in type 1 diabetes. Brain Res 946:221–231
50. Kerr JF (2024) Introduction Definition Of Apoptosis And Overview Of Its Incidence, Programmed cell death. CRC, pp 1–15
51. Sivasinprasasn S, Tocharus J, Mahatheeranont S, Nakrat S, Tocharus C (2024) Anthocyanin-Rich Fraction of Black Rice Bran Extract Protects against Amyloid β-Induced Oxidative Stress, Endoplasmic Reticulum Stress, and Neuronal Apoptosis in SK-N-SH Cells. Pharmaceuticals 17:1039
52. Duan X-K, Sun Y-X, Wang H-Y, Xu Y-Y, Fan S-Z, Tian J-Y, Yu Y, Zhao Y-Y, Jiang Y-L (2023) miR-124 is upregulated in diabetic mice and inhibits proliferation and promotes apoptosis of high-glucose-induced β-cells by targeting EZH2. World J Diabetes 14:209

Publisher's note Springer Nature remains neutral with regard to jurisdictional claims in published maps and institutional affiliations.

Springer Nature or its licensor (e.g. a society or other partner) holds exclusive rights to this article under a publishing agreement with the author(s) or other rightsholder(s); author self-archiving of the accepted manuscript version of this article is solely governed by the terms of such publishing agreement and applicable law.

SPRINGER NATURE Link

Log in

Menu Search Cart

Home Molecular Biology Reports Articles



Molecular Biology Reports

Publishing model: **Hybrid**

Save journal

View saved research

Atatürk University Great news! Funding is available for open access publishing.

Explore open access funding Change institution

Journal menu

Articles

Search all Molecular Biology Reports articles →

Filter by

Volume:

All volumes

Publishing model:

☐ Open access only

Sort by

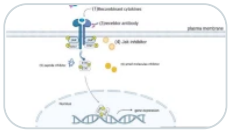
Date published:

◯ New to old ◯ Old to new

Update results

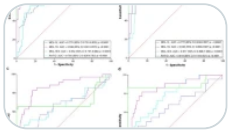
Showing 1–50 of 14,097 articles

The *JAK/STAT* pathway: key mechanism in gene activation, disease regulation, and emerging therapeutic targets



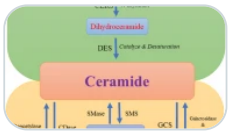
Review | 09 May 2026 | Article: 732

Host mitochondrial apoptotic signatures in children with chronic conditions reveal viral modulation of MCL-1 in severe SARS-CoV-2 infection



Original Article | Open access | 09 May 2026 | Article: 731

Curcumin as a ceramide metabolism-targeting agent: Molecular mechanisms and therapeutic implications in cancer



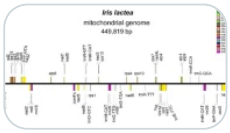
Review | 08 May 2026 | Article: 730

The importance of phagocytosis and its effect on the immune system



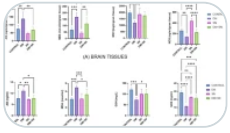
Review | 08 May 2026 | Article: 729

Comparative analysis of mitochondrial genomes of *Iris lactea* reveals gene transfer and RNA-editing events



Original Article | 08 May 2026 | Article: 728

Neuroprotective effects of black elderberry (*Sambucus nigra*) extract through the role of miR-124-5p and miR-144-5p in a streptozotocin-induced Type 2 diabetic rat model



Original Article | 08 May 2026 | Article: 727

Part of 1 collection:

Diabetes

Research progress on the roles and mechanisms of flavonoid monomers in liver diseases: a review



Review | 08 May 2026 | Article: 726

Part of 1 collection:

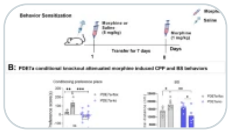
Digestive Diseases

Targeting the APE1 hub: integrating DNA repair and redox signaling for precision management of inflammation-associated diseases



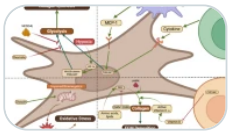
Mini Review | 07 May 2026 | Article: 725

Neuronal deletion of PDE7A averts morphine-induced behavioral plasticity and impairs downstream AKT signaling



Original Article | 07 May 2026 | Article: 724

Metabolic reprogramming and ferroptosis in keloid pathogenesis: new insights for targeted therapy

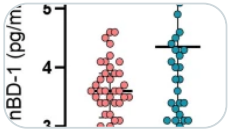


Review | 07 May 2026 | Article: 723

Part of 1 collection:

Extracellular Matrix Biology

Exploratory study of *DEFB1* genetic variants and human β-defensin-1 expression in monosodium urate crystal–induced arthritis: insights into innate immune regulation



Original Article | 07 May 2026 | Article: 722

Correction: The Dual Roles of TIMP-1 in Cancer: From Protease Inhibition to Cytokine Signaling

Correction | 07 May 2026 | Article: 721

Extracellular vesicles in ophthalmology: innovations in diagnosis, therapy, and drug delivery



Review | 06 May 2026 | Article: 720

CRISPR/Cas9 in perspective: evaluating efficacy, delivery methods, and ethical challenges in genome editing



Review | 06 May 2026 | Article: 719

Genetic modulation of pain pathways: toward a new era in pain therapy- a systematic review



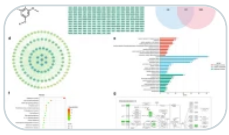
Review | 06 May 2026 | Article: 718

RNA methylation in cardiovascular remodeling: Molecular mechanisms, biomarkers, and therapeutic strategies



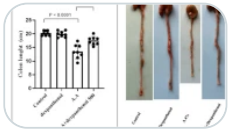
Review | 05 May 2026 | Article: 717

Cardamonin activates AMPK/FOXO3a/Nrf-2 axis to ameliorate oxidative stress in hyperlipidemia induced cardiac injury in mice



Original Article | 05 May 2026 | Article: 716

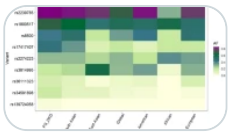
Dexpanthenol reduces IL 6 and VEGF gene expression in a rat model of acetic acid induced ulcerative colitis



Original Article | 05 May 2026 | Article: 715

Part of 1 collection:
Digestive Diseases

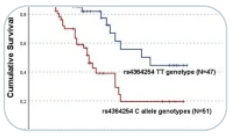
Multi-variant genotyping identifies association of TRPC6 rs36111323 with diabetic kidney disease in a South Indian population



Original Article | 05 May 2026 | Article: 714

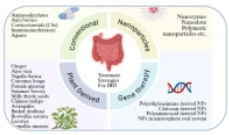
Part of 1 collection:
Diabetes

Heparanase (HPSE) genetic variants as prognostic indicators in ovarian cancer: evidence from discovery and validation cohorts



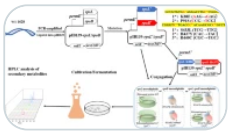
Original Article | Open access | 05 May 2026 | Article: 713

Multi-modal therapeutic approaches to inflammatory bowel disease: plant-derived compounds, nanoparticle drug delivery systems, and gene-based interventions



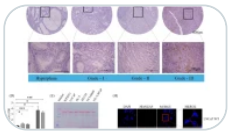
Review | 05 May 2026 | Article: 712

Rational construction of *rpsL* or/and *rpoB* merodiploids affects biosynthesis of secondary metabolite in *Streptomyces*



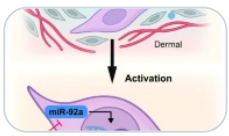
Original Article | 05 May 2026 | Article: 711

Oncogenic MAGEA4 directs neuroendocrine differentiation and survival in prostate cancer cells through the SIRT1/Acetyl-p53/BCL-2 axis



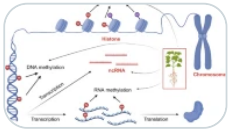
Original Article | 05 May 2026 | Article: 710

Astragalus polysaccharide accelerates wound healing by targeting the miR-92a/FGF2 axis in dermal fibroblasts



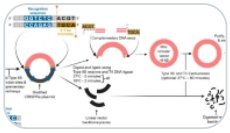
Original Article | 02 May 2026 | Article: 709

Research progress on active components from natural medicines inhibiting tumor via epigenetic regulation



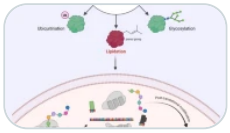
Review | 02 May 2026 | Article: 708

Miniaturization of CRISPRa plasmids for efficient delivery into renal epithelial cells and *Pkd1* transactivation



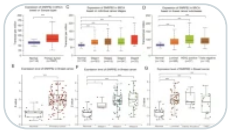
Original Article | 02 May 2026 | Article: 707

The role of protein prenylation in kidney diseases: Molecular basis and therapeutic implications



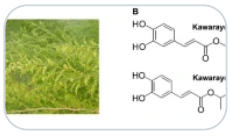
Review | 02 May 2026 | Article: 706

Emerging roles for SNRPB2 in governing the cell cycle and steering tumor immune modulation in breast cancer



Original Article | Open access | 02 May 2026 | Article: 705

Epigenetic regulation of hyaluronan degradation and melanogenesis by Kawarayomogin I and II from *Artemisia capillaris* via miR-486-5p and miR-141-3p



Brief Report | 02 May 2026 | Article: 704

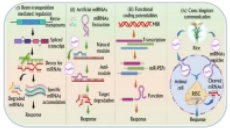
Insulin resistance, inflammation, oxidative stress and dysregulated WNT/β-Catenin signaling in polycystic ovary syndrome: A review



Review | 30 April 2026 | Article: 703

Part of 1 collection:
Reproductive Biology

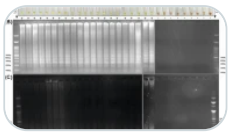
Recent advances in miRNAs mediated agronomical advantageous traits improvement in rice



Review | 30 April 2026 | Article: 702

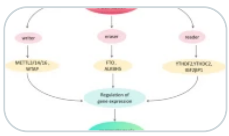
Part of 1 collection:
Plant Molecular Biology

Rapid and visually interpretable LAMP assay for detection of pathogenic *Pseudomonas aeruginosa* in artificial sputum



Original Article | 30 April 2026 | Article: 701

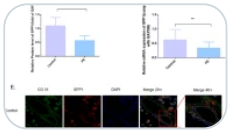
The role of m6A modification in spermatogenic dysfunction



Mini Review | 30 April 2026 | Article: 700

Part of 1 collection:
Reproductive Biology

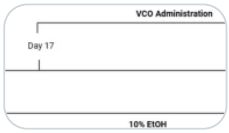
SPP1 integrates trophoblast-endothelial crosstalk via the αVβ3–PI3K/Akt–MMP-9 axis to govern vascular remodeling in preeclampsia



Original Article | Open access | 30 April 2026 | Article: 699

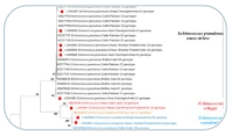
Part of 1 collection:
Reproductive Biology

Neurotrophic and metabolic consequences of virgin coconut oil and ethanol: implications for growth and antioxidant defense



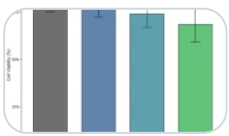
Original Article | 29 April 2026 | Article: 698

Mitochondrial *nad5* gene-based genetic diversity analysis of *Echinococcus granulosus* sensu lato hydatid cysts in small ruminants of north India



Original Article | 29 April 2026 | Article: 697

Effect of irisin on miRNA-associated changes in the PGC-1α/FNDC5/BDNF Axis in an in vitro model of MPP^+-induced Parkinson's



disease

Original Article | 29 April 2026 | Article: 696

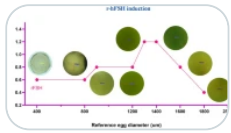
Beyond CRISPR/Cas9: emerging genome editing technologies for next-generation crop improvement



Review | 29 April 2026 | Article: 695

Part of 1 collection:
Plant Molecular Biology

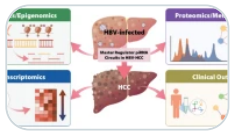
Macromolecular interactions of recombinant human follicle stimulating hormone (r-hFSH) with piscine FSH receptors enhance reproductive development in *Clarias magur*: in silico data corroborated by an in vivo study



Original Article | 29 April 2026 | Article: 694

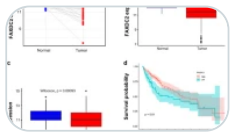
Part of 1 collection:
Reproductive Biology

Beyond silencing: integrative multi-omics and spatial profiling unravel the systems-level role of piRNAs in HBV-driven Hepatocarcinogenesis



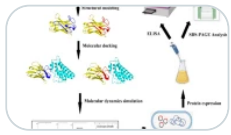
Review | 29 April 2026 | Article: 693

Knockdown of FAXDC2 promotes cell proliferation, migration, invasion and EMT in HepG2 cells by upregulating c-Met and its phosphorylation



Original Article | 29 April 2026 | Article: 692

Molecular dynamics simulations along with the synthesis of innovative engineered nanobodies targeting Interleukin-2



Original Article | 29 April 2026 | Article: 691

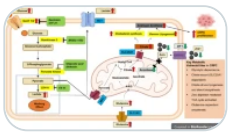
A novel de novo frameshift variant in *ZMYM2* expands the neuropsychiatric spectrum of NECRC syndrome: a case report



Case Report | 29 April 2026 | Article: 690

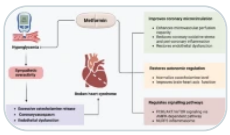
Part of 1 collection:
Neuroscience

Rewired lipid metabolism in castration-resistant prostate cancer: molecular interplay between glucose metabolism and sterol synthesis



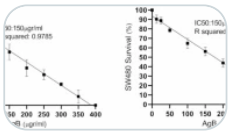
Review | 28 April 2026 | Article: 689

Metformin as a potential therapeutic agent in broken heart syndrome: Targeting AMPK-dependent cardio-protection and microvascular function



Review | 28 April 2026 | Article: 688

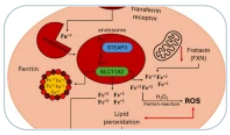
Hydatid cyst antigen B: inducer of inflammatory and apoptotic responses in colon cancer cell lines (SW480 and SW948)



Original Article | 28 April 2026 | Article: 687

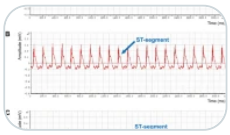
Part of 1 collection:
Digestive Diseases

The role of estrogen and its receptors in the regulation of ferroptosis and autophagy



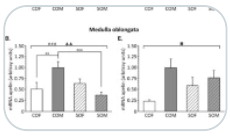
Review | Open access | 28 April 2026 | Article: 686

Knockdown of Transthyretin ameliorates ferroptosis in myocardial ischemia-reperfusion injury



Original Article | 28 April 2026 | Article: 685

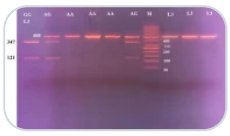
Sex-related expression of apelin/APJ in the adolescent and adult rat offspring exposed to maternal peripartum depression



Brief Report | 28 April 2026 | Article: 684

Part of 1 collection:
Neuroscience

IL-27−964 A/G polymorphism promoter polymorphism, serum IL-27, and vitamin D in multiple sclerosis: evidence from an egyptian case–control study



Original Article | 28 April 2026 | Article: 683

1 2 ... 282 Next >

MOLECULAR BIOLOGY REPORTS

ISSN
0301-4851

EISSN
1573-4978

JCR ABBREVIATION
MOL BIOL REP

ISO ABBREVIATION
Mol. Biol. Rep.

Journal information

EDITION
Science Citation Index Expanded (SCIE)

CATEGORY
BIOCHEMISTRY & MOLECULAR BIOLOGY

LANGUAGES
English

REGION
NETHERLANDS

1ST ELECTRONIC JCR YEAR
1997

Publisher information

PUBLISHER
SPRINGER

ADDRESS
VAN GODEWIJCKSTRAAT 30, 3311 GZ DORDRECHT, NETHERLANDS

PUBLICATION FREQUENCY
12 issues/year

Journal’s performance

Journal Impact Factor

The Journal Impact Factor (JIF) is a journal-level metric calculated from data indexed in the Web of Science Core Collection. It should be used with careful attention to the many factors that influence citation rates, such as the volume of publication and citations characteristics of the subject area and type of journal. The Journal Impact Factor can complement expert opinion and informed peer review. In the case of academic evaluation for tenure, it is inappropriate to use a journal-level metric as a proxy measure for individual researchers, institutions, or articles. Learn more

2024 JOURNAL IMPACT FACTOR
2.8
View calculation

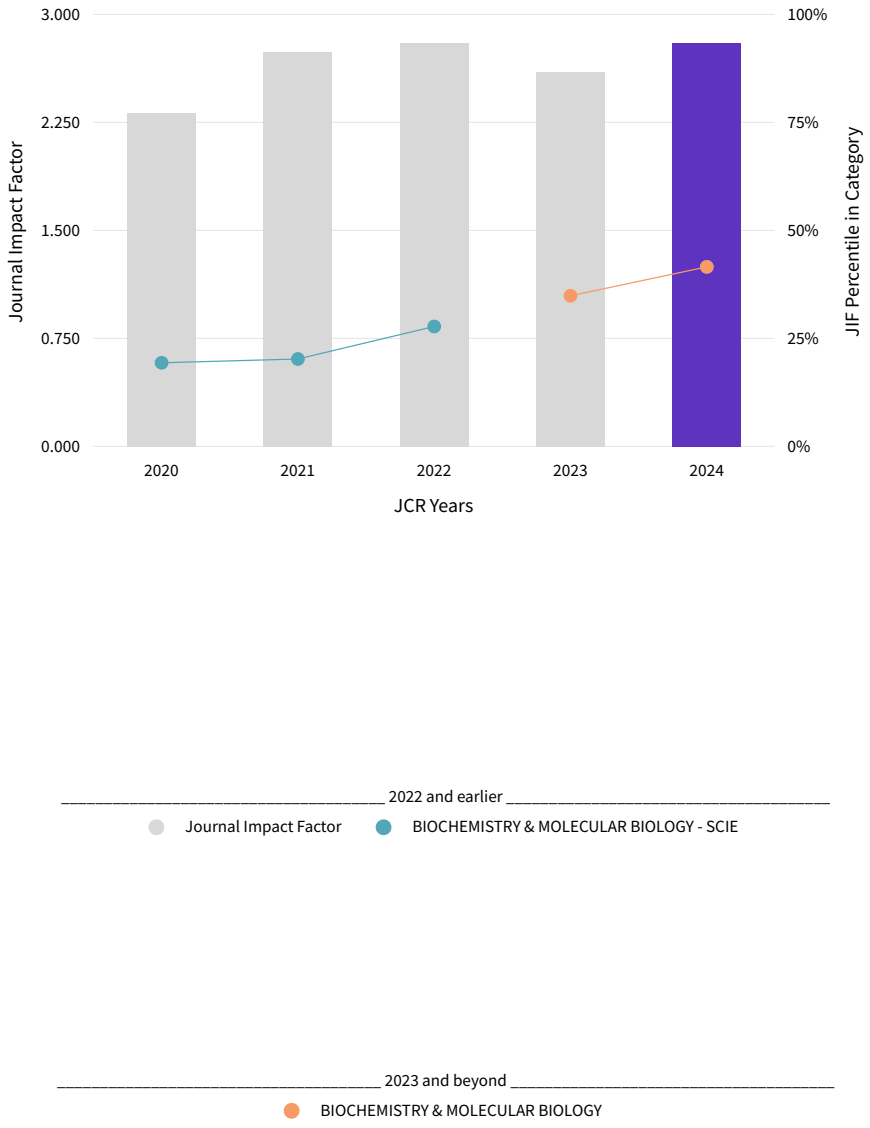
JOURNAL IMPACT FACTOR WITHOUT SELF CITATIONS
2.8
View calculation

Journal Impact Factor Trend 2024 Export

Journal Impact Factor contributing items Export

Citable items (1,851) Citing Sources (1,721)

TITLE	CITATION COUNT
DNA barcoding, an effective tool for species identification: a review	66



Cancer treatment therapies: traditional to modern approaches to combat…	62
Interplay between PI3K/AKT pathway and heart disorders	44
Breast cancer in the era of precision medicine	37
Biomarkers of liver diseases	35
The cell cycle, cancer development and therapy	33
Role and relevance of fish cell lines in advanced in vitro research	25
The role of hypoxia on prostate cancer progression and metastasis	25
Advances in siRNA delivery approaches in cancer therapy: challenges and…	24
The deadly cross-talk between Hippo pathway and epithelial-mesenchyma…	24

View All in Web of Science

View all years

Journal Citation Indicator (JCI)

Export

0.48

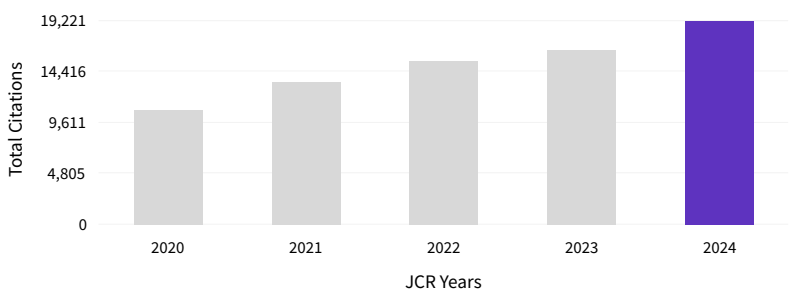
The Journal Citation Indicator (JCI) is the average Category Normalized Citation Impact (CNCI) of citable items (articles & reviews) published by a journal over a recent three year period. The average JCI in a category is 1. Journals with a JCI of 1.5 have 50% more citation impact than the average in that category. It may be used alongside other metrics to help you evaluate journals. Learn more

Total Citations

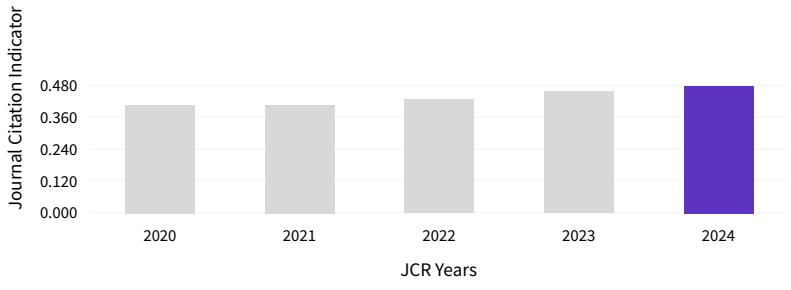
Export

19,221

The total number of times that a journal has been cited by all journals included in the database in the JCR year. Citations to journals listed in JCR are compiled annually from the JCR years combined database, regardless of which JCR edition lists the journal.



View all years



View all years

Citation distribution

Export

The Citation Distribution shows the frequency with which items published in the year or two years prior were cited in the JCR data year (i.e., the component of the calculation of the JIF). The graph has similar functionality as the JIF Trend graph, including hover-over data descriptions for each data point, and an interactive legend where each data element's legend can be used as a toggle. You can view Articles, Reviews, or Non-Citable (other) items to the JIF numerator. Learn more

ARTICLE CITATION MEDIAN

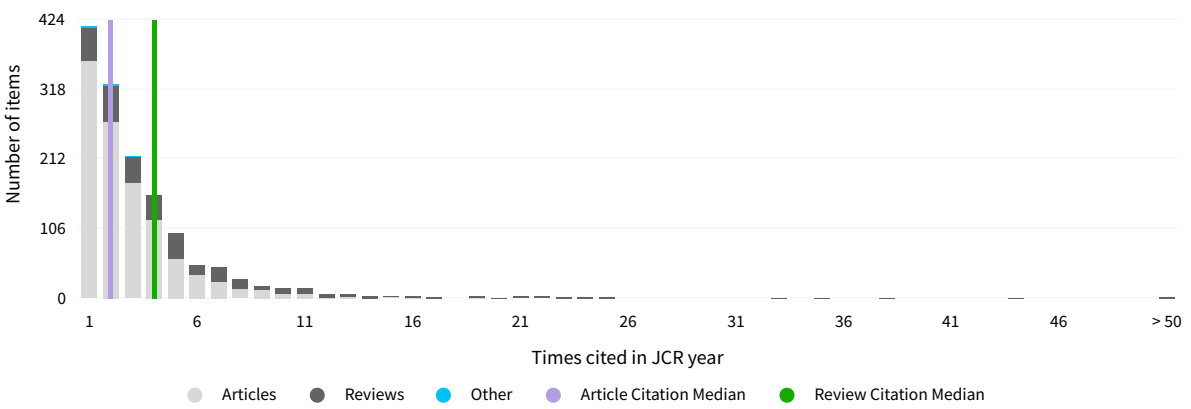
2

REVIEW CITATION MEDIAN

4

UNLINKED CITATIONS

27



TIMES CITED

0

ARTICLES

369

REVIEWS

43

OTHER

52

Open Access (OA)

Export

The data included in this tile summarizes the items published in the journal in the JCR data year and in the previous two years. This three-year set of published items is used to provide descriptive analysis of the content and community of the journal. Learn more

Items

TOTAL CITABLE	% OF CITABLE OA
2,974	11.00%

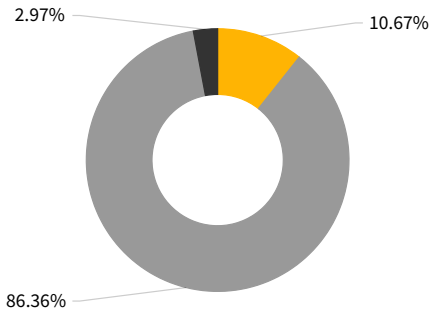
Citations*

TOTAL CITABLE	% OF CITABLE OA
6,264	13.78%

CITABLE

GOLD OPEN ACCESS
327 / 10.67%

SUBSCRIPTION AND FREE TO READ
2,647 / 86.36%



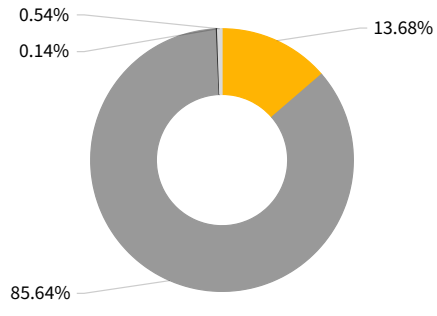
NON-CITABLE

OTHER (NON CITABLE ITEMS)
91 / 2.97%

CITABLE

GOLD OPEN ACCESS
863 / 13.68%

SUBSCRIPTION AND FREE TO READ
5,401 / 85.64%



NON-CITABLE

OTHER (NON CITABLE ITEMS)
9 / 0.14%

UNLINKED CITATIONS
34 / 0.54%

*Citations in 2024 to items published in [2022 - 2024]

Rank by Journal Impact Factor

Journals within a category are sorted in descending order by Journal Impact Factor (JIF) resulting in the Category Ranking below. A separate rank is shown for each category in which the journal is listed in JCR. Beginning in 2023, ranks are calculated by category. Learn more

CATEGORY
BIOCHEMISTRY & MOLECULAR BIOLOGY

187/320

JCR YEAR	JIF RANK	JIF QUARTILE	JIF PERCENTILE
2024	187/320	Q3	41.7
2023	204/313	Q3	35.0

Rank by JIF before 2023 for BIOCHEMISTRY & MOLECULAR BIOLOGY

EDITION
Science Citation Index Expanded (SCIE)

JCR YEAR	JIF RANK	JIF QUARTILE	JIF PERCENTILE
2022	206/285	Q3	27.9
2021	237/297	Q4	20.37
2020	238/295	Q4	19.49

Rank by Journal Citation Indicator (JCI)

Journals within a category are sorted in descending order by Journal Citation Indicator (JCI) resulting in the Category Ranking below. A separate rank is shown for each category in which the journal is listed in JCR. Data for the most recent year is presented at the top of the list, with other years shown in reverse chronological order. Learn more

CATEGORY

BIOCHEMISTRY & MOLECULAR BIOLOGY

241/321

JCR YEAR	JCI RANK	JCI QUARTILE	JCI PERCENTILE
2024	241/321	Q4	25.08
2023	245/313	Q4	21.88
2022	251/315	Q4	20.48
2021	248/322	Q4	23.14
2020	248/311	Q4	20.42
2019	264/310	Q4	15.00
2018	210/308	Q3	31.98

Citation network

Cited Half-life

4.1 years

The Cited Half-Life is the median age of the items in this journal that were cited in the JCR year. Half of a journal's cited items were published more recently than the cited half-life.

TOTAL NUMBER OF CITES

19,221

NON SELF-CITATIONS

18,918

SELF-CITATIONS

303

Citing Half-life

7.1 years

The Citing Half-Life is the median age of items in other publications cited by this journal in the JCR year.

TOTAL NUMBER OF CITES

64,082

NON SELF-CITATIONS

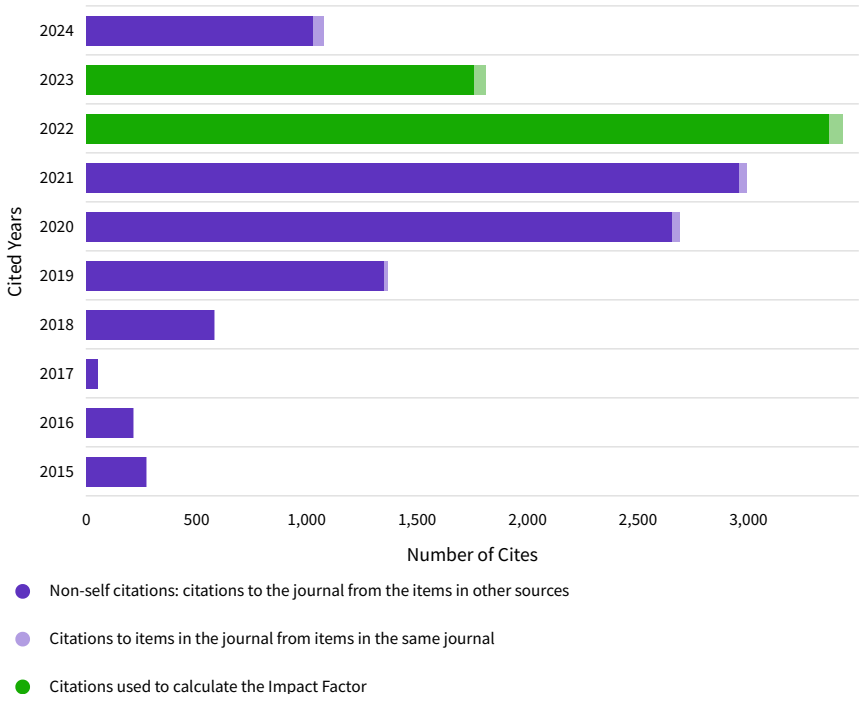
63,779

SELF-CITATIONS

303

Cited Half-life Data | Citing Half-life Data

Export

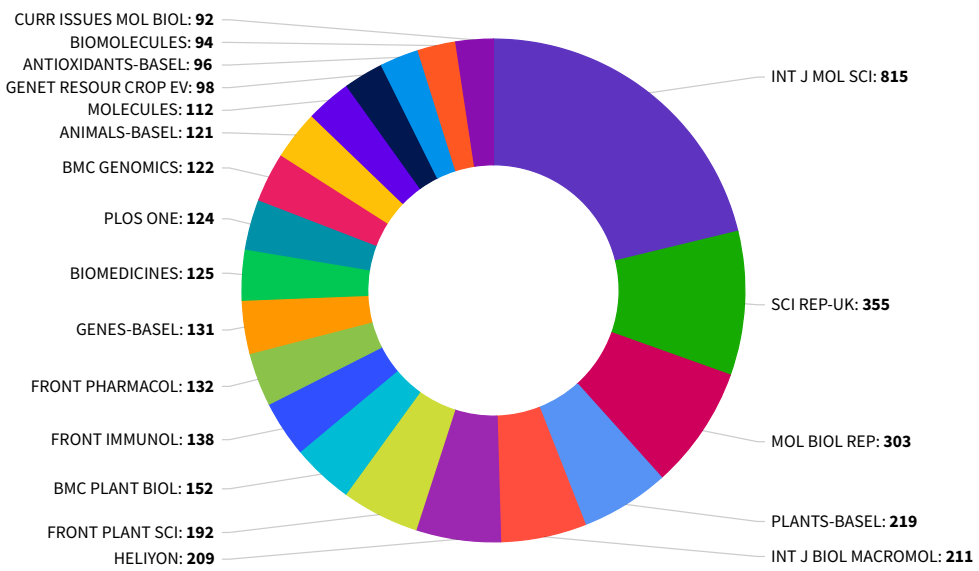


CITED YEAR	# OF CITES FROM 2024	CUMULATIVE %	# OF CITING SOURCES
All years	**19,221 citations**	**100.00%**	**3,371 sources**
2024	1,075 citations	5.59%	557 sources
2023	1,808 citations	15.00%	873 sources
2022	3,424 citations	32.81%	1,333 sources
2021	2,989 citations	48.36%	1,272 sources
2020	2,689 citations	62.35%	1,185 sources
2019	1,366 citations	69.46%	724 sources
2018	582 citations	72.49%	410 sources
2017	52 citations	72.76%	49 sources
2016	213 citations	73.87%	158 sources
2015	271 citations	75.28%	198 sources
Older	4,752 citations		

Journal Citation Relationships

Cited Data | Citing Data

Top 20 journals citing MOL BIOL REP by number of citations



Content metrics

Source data

This tile shows the breakdown of document types published by the journal. Citable Items are Articles and Reviews. For the purposes of calculating JIF, a JCR year considers the publications of that journal in the two prior years. Learn more

1,123 total citable items

	ARTICLES	REVIEWS	COMBINED(C)	OTHER DOCUMENT TYPES(O)	PERCEI
NUMBER IN JCR YEAR 2024 (A)	877	246	1,123	42	96%
NUMBER OF REFERENCES (B)	38,273	25,733	64,006	76	100%
RATIO (B/A)	43.6	104.6	57.0	1.8	

Average JIF Percentile

Export

The Average Journal Impact Factor Percentile takes the sum of the JIF Percentile rank for each category under consideration, then calculates the average of those values. Learn more

ALL CATEGORIES AVERAGE
41.7

BIOCHEMISTRY & MOLECULAR BIOLOGY
41.7

Contributions by organizations

Export

Organizations that have contributed the most papers to the journal in the most recent three-year period. Learn more

RANK	ORGANIZATION	COUNT
1	INDIAN COUNCIL OF AGRICULTURAL RESEARCH (ICAR)	107
-	ISLAMIC AZAD UNIVERSITY	107
3	EGYPTIAN KNOWLEDGE BANK (EKB)	106
4	SHAHID BEHESHTI UNIVERSITY MEDICAL SCIENCES	95
5	TEHRAN UNIVERSITY OF MEDICAL SCIENCES	77

Contributions by country/region

Export

Countries or Regions that have contributed the most papers to the journal in the most recent three-year period. Learn more

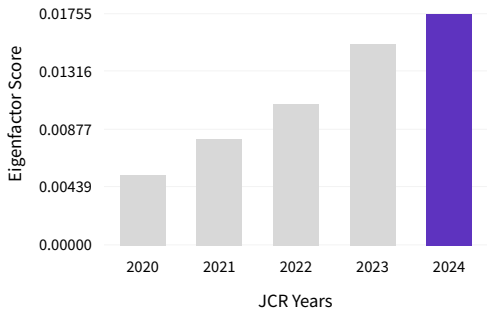
RANK	COUNTRY / REGION	COUNT
1	CHINA MAINLAND	835
2	INDIA	589
3	IRAN	555
4	TURKIYE	254
5	USA	203
6	PAKISTAN	142
7	EGYPT	108
8	BRAZIL	101
9	SAUDI ARABIA	87

Additional metrics

Eigenfactor Score

0.01755

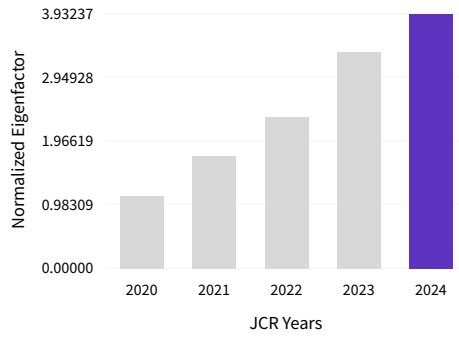
The Eigenfactor Score is a reflection of the density of the network of citations around the journal using 5 years of cited content as cited by the Current Year. It considers both the number of citations and the source of those citations, so that highly cited sources will influence the network more than less cited sources. The Eigenfactor calculation does not include journal self-citations. Learn more



Normalized Eigenfactor

3.93237

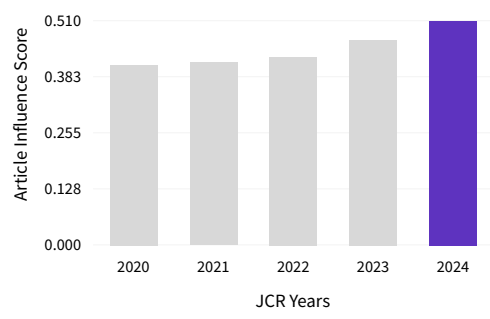
The Normalized Eigenfactor Score is the Eigenfactor score normalized, by rescaling the total number of journals in the JCR each year, so that the average journal has a score of 1. Journals can then be compared and influence measured by their score relative to 1. Learn more



Article influence score

0.510

The Article Influence Score normalizes the Eigenfactor Score according to the cumulative size of the cited journal across the prior five years. The mean Article Influence Score for each article is 1.00. A score greater than 1.00 indicates that each article in the journal has above-average influence. Learn more



5 Year Impact Factor

2.8

View Calculation

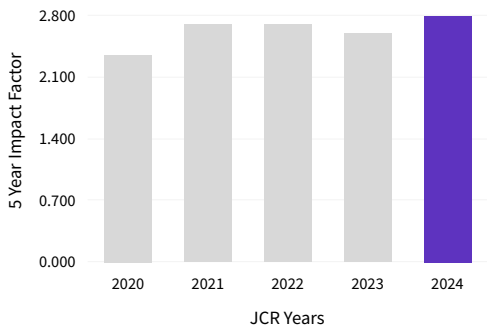
The 5-year Impact Factor is the average number of times articles from the journal published in the past five years have been cited in the JCR year. It is calculated by dividing the number of citations in the JCR year by the total number of articles published in the five previous years. Learn more

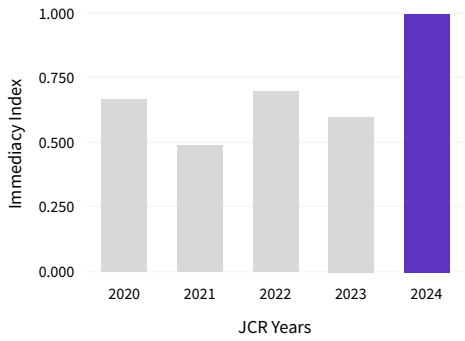
Immediacy Index

1.0

View Calculation

The Immediacy Index is the count of citations in the current year to the journal that reference content in this same year. Journals that have a consistently high Immediacy Index attract citations rapidly. Learn more





© 2026 Clarivate
Legal center
Privacy notice
Cookie policy
Terms of Use
Manage cookie preferences
Copyright notice
Accessibility
Help

SPRINGER NATURE Link

Log in

Menu Search Cart

Home Molecular Biology Reports Editorial board

Molecular Biology Reports

Publishing model: Hybrid

Save journal

View saved research

Atatürk University

Great news! Funding is available for open access publishing.

Explore open access funding Change institution

Journal menu

Editorial board

Editors-In-Chief

Rodrigo Guimarães PhD
Independent Researcher, South Holland, The Netherlands

Gillian E. Knight PhD
Independent Researcher, London, United Kingdom

Deputy Editors-in-Chief

Neeti Sanan-Mishra PhD
International Centre for Genetic Engineering and Biotechnology, New Delhi, India

Ya-Qun Zhou PhD
Tongji Hospital, Huazhong University of Science and Technology Hospital, Wuhan, China

Section Editor - Diabetes

Simranjeet Kaur MSc, PhD
Steno Diabetes Center Copenhagen, Herlev, Denmark

Sally Kent PhD
University of Massachusetts Chan Medical School, Worcester, United States

Xiangwei Xiao PhD
University of Pittsburgh, Pittsburgh, United States

Section Editor – Extracellular Matrix Biology

Valerio Izzi PhD
University of Oulu, Oulu, Finland

Nikos Karamanos PhD
University of Patras, Pátrai, Greece

Hiroshi Kitagawa PhD
Kobe Pharmaceutical University, Kobe, Japan

Alberto Passi PhD
University of Insubria, Varese, Italy

Irit Sagi PhD
Weizmann Institute of Science, Rehovot, Israel

Sarah Wilcox-Adelman PhD
Matrix Biology Institute, Edgewater, United States

Section Editors – Neuroscience

Marija Cvetanovic PhD
University of Minnesota, Minneapolis, United States

Md Nabiul Islam PhD
Yamaguchi University, Yamaguchi, Japan

Olga Kopach PhD
University College London, London, United Kingdom

Sabine Liebscher PhD
University of Cologne, Cologne, Germany

Dai-Qiang Liu PhD
Huazhong University of Science and Technology Hospital, Wuhan, China

Caroline Ran PhD
Karolinska Institutet, Stockholm, Sweden

Sumit Sarkar PhD
National Center for Toxicological Research, Pine Bluff, United States

Smita Saxena PhD
University of Missouri, Columbia, United States

Xiaopu Zhou PhD
Hospital for Sick Children, Toronto, Canada

Section Editors – Plant Molecular Biology

Charith Raj Adkar-Purushothama PhD
Université de Sherbrooke, Sherbrooke, Canada

Zahir Ali PhD
King Abdullah University of Science and Technology, Jeddah, Saudi Arabia

Qingzhang Du, Dr. Sci.(Biol.)
Beijing Forestry University, Beijing, China

Ajit Ghosh PhD
Shahjalal University of Science and Technology, Sylhet, Bangladesh

Benjamin Karikari PhD
Université Laval, Québec, Canada

Dongfang Ma PhD
Yangtze University, Jingzhou, China

Richard Magwanga, Dr. Sci. (Biol.)
Jaramogi Oginga Odinga University of Science and Technology, Bondo, Kenya

Ajay Kumar Pandey PhD
National Agri-Food Biotechnology Institute, Mohali, India

Gunvant Patil PhD
Texas Tech University, Lubbock, United States

Mingyang Quan PhD
Beijing Forestry University, Beijing, China

Dinesh Kumar Saini PhD
Texas Tech University, Lubbock, United States

Ahmed Sallam PhD
Assiut University, Asyut, Egypt

Rahul Mahadev Shelake PhD
Gyeongsang National University, Jinju-si, South Korea

Qiang Wei PhD
Nanjing Forestry University, Nanjing, China

Qiaoli Xie PhD
Chongqing University, Chongqing, China

Yongliang Zhang PhD
China Agricultural University, Beijing, China

Associate Editors

Ritu Chaudhary PhD
Center for Cancer Research, Bethesda, United States

Nitish Gulve PhD
The Wistar Institute, Philadelphia, United States

Deepak Parashar PhD
Medical College of Wisconsin, Milwaukee, United States

Raghuveer Singh PhD
University of Florida, Gainesville, United States

Section Editors - Antimicrobial Resistance

Izzet Burcin Saticioglu DVM, PhD
Bursa Uludağ Üniversitesi, Bursa, Türkiye

Section Editors - Immune Cells

Kevin Chih-Yang Huang PhD
China Medical University, Taichung, Taiwan

Arong Gaowa PhD
Mie University, Tsu, Japan

Aisha Naeem PhD
Qatar University, Doha, Qatar

Editorial Board

Amina Abbadi PhD
Harvard University, Cambridge, United States

Sarah Abou Alaiwi PhD
Dana-Farber Cancer Institute, Boston, United States

Laura Alaniz PhD
National University of Northwestern Buenos Aires, Junín, Argentina

Arnab Banerjee PhD
Serampore College, Serampore, India

Abeni Beshiru PhD, MSc, BSc
Western Delta University, Asaba, Nigeria

Ramray Bhat PhD
Indian Institute of Science Bangalore, Bengaluru, India

Srinivasa Reddy Bonam PhD
CSIR, Indian Institute of Chemical Technology, Hyderabad, India

Nishant Chakravorty PhD
Indian Institute of Technology Kharagpur, Kharagpur, India

Alexandra Chittka PhD
University College London, London, United Kingdom

Altino Choupina PhD
Polytechnic Institute of Bragança, Bragança, Portugal

Natália Cruz-Martins PhD
i3S - Instituto de Investigação e Inovação em Saúde, Universidade do Porto, Porto, Portugal

Nishant A. Dafale, Dr. Sci. (Microbiology), PhD
National Environmental Engineering Research Institute, Nagpur, India

Vijaya Kumar Deekshit PhD
Nitte University, Mangaluru, India

Praveen Kumar Dubey PhD
University of Alabama, Tuscaloosa, United States

Laurent Duca PhD
Université de Reims Champagne-Ardenne, Reims, France

Sadeesh E M PhD
National Dairy Research Institute, Karnāl, India

Yingmei Feng PhD
Capital Medical University, Beijing, China

Karin Forsberg-Nilsson PhD
University of Nottingham, Nottingham, United Kingdom; Uppsala University, Uppsala, Sweden

Marco Franchi PhD

University of Bologna, Bologna, Italy

Arit Ghosh PhD
University of California San Diego, San Diego, United States

Chrysostomi Gialeli PhD
Lund University, Lund, Sweden

Martin Götte PhD
University Hospital Münster, Münster, Germany

Elon Donald Gullberg PhD
University of Bergen, Bergen, Norway

Himanshu Gupta PhD
London School of Hygiene & Tropical Medicine, London, United Kingdom

Paraskevi Heldin PhD
Uppsala University, Uppsala, Sweden

Renato V. Iozzo PhD
Thomas Jefferson University, Philadelphia, United States

Xijian Ke MD
Huazhong University of Science and Technology, Wuhan, China

Dimitris Kletsas PhD
National Centre of Scientific Research "Demokritos", Athens, Greece

Ilona Kovalszky PhD
Semmelweis University, Budapest, Hungary

Shardul Kulkarni PhD
National Institutes of Health, Bethesda, United States

Shruti Lal PhD
University of Southern California, Los Angeles, United States

Dawei Li PhD
Pennsylvania State University, State College, United States

Feng Li MD, PhD
University of Pittsburgh, Pittsburgh, United States

Liming Li PhD
Princeton University, Princeton, United States

Weibiao Liao PhD
Gansu Agricultural University, Lanzhou, China

Guangliang Liu PhD
Chinese Academy of Agricultural Sciences, Beijing, China

Shikai Liu PhD
Ocean University of China, Qingdao, China

Ida Gjervold Lunde PhD
Akershus University Hospital, Lillestrøm, Norway

Hongyu Ma PhD
Shantou University, Shantou, China

Ana Magalhães PhD
Universidade do Porto, Porto, Portugal

Fransiska Malfait PhD
Ghent University Hospital, Ghent, Belgium

Valentina Masola PhD
University of Padua, Padua, Italy

Albert Sleiman Mellick PhD
UNSW Sydney, Sydney, Australia

Shuzhen Men PhD
Nankai University, Tianjin, China

Maria Mirabelli PhD
Magna Graecia University, Catanzaro, Italy

Suniti Misra PhD
Medical University of South Carolina, Charleston, United States

Sibin M K PhD
Armed Forces Medical College, Pune, India

Abdel Moneim PhD
Helwan University, Cairo, Egypt

Muhammad Azhar Nadeem PhD
Sivas Bilim ve Teknoloji Üniversitesi, Sivas, Türkiye

Amin Nassar PhD
Harvard University, Cambridge, United States

Dragana Nikitovic PhD
University of Crete, Rethymno, Greece

Oommen Podiyan Oommen PhD
Tampere University, Tampere, Finland

Gertraud Orend PhD
Hôpital Civil, Strasbourg, Strasbourg, France

Veronique Orian-Rousseau PhD
Karlsruhe Institute of Technology, Karlsruhe, Germany

Narisimham Parinandi PhD
The Ohio State University Wexner Medical Center, Columbus, United States

Fernando Rodríguez Pascual PhD
Universidad Autónoma de Madrid, Madrid, Spain

Mauro Sérgio Gonçalves Pavão PhD
Universidade Federal do Rio de Janeiro, Rio de Janeiro, Brazil

Huan Peng PhD
Chinese Academy of Agricultural Sciences, Beijing, China

Alexander Pietras PhD
Lund University, Lund, Sweden

David John Pocock PhD

Monash University, Melbourne, Australia

Aurel Popa-Wagner PhD
Griffith University, Brisbane, Australia

Fabio Quondamatteo PhD
Royal College of Surgeons in Ireland, Dublin, Ireland

Mingchun Ren PhD
Chinese Academy of Fishery Sciences, Beijing, China

Sylvie Ricard-Blum PhD
Université Claude Bernard Lyon 1, Villeurbanne, France

Kirsi Rilla PhD
University of Eastern Finland, Kuopio, Finland

Antonio Rossi PhD
University of Pavia, Pavia, Italy

Patricia Rousselle PhD
Centre National de la Recherche Scientifique, Paris, France

Rashmin C. Savani PhD
The University of Texas Southwestern Medical Center, Dallas, United States

Liliana Schaefer PhD
Goethe University Frankfurt, Frankfurt am Main, Germany

Andreas Scorilas PhD
National and Kapodistrian University of Athens, Athens, Greece

Tripti Sharma PhD
The University of Texas Southwestern Medical Center, Dallas, United States

Vikas Sharma PhD
Sant Baba Bhag Singh University Jalandhar, Jalandhar, India

Yuuki Shimizu PhD
Nagoya University, Nagoya, Japan

Kai Shu PhD
Northwestern Polytechnical University, Xi'an, China

Anna Stejskalova PhD
Harvard University, Cambridge, United States

Jianmin Sun PhD
Ningxia Medical University, Yinchuan, China

Yuan-Xiang Tao PhD
Rutgers, The State University of New Jersey, New Brunswick, United States

Achilleas Theocharis PhD
University of Patras, Pátrai, Greece

Ramesha Thimmappa PhD
Amity University, Noida, India

Linda Troeberg PhD
University of East Anglia, Norwich, United Kingdom

Lilla Turiak PhD
Hungarian Research Network, Budapest, Hungary

Boris Turk PhD
Jožef Stefan Institute, Ljubljana, Slovenia

Ali Vaziri-Gohar PhD
Case Western Reserve University, Cleveland, United States

Praveen Vikas PhD
University of Iowa, Iowa City, United States

Jean-Baptiste Vincourt PhD
Université de Lorraine, Nancy, France

Huiwen Wang PhD
Chinese Academy of Sciences, Beijing, China

Zhenye Yang PhD
University of Science and Technology of China, Hefei, China

Frank Zaucke PhD
Goethe University Frankfurt, Frankfurt am Main, Germany

Dimitrios I. Zeugolis PhD
University College Dublin, Dublin, Ireland

Chengfei Zhang PhD
University of Hong Kong, Pok Fu Lam, Hong Kong

Kai Zhang PhD
University of California, Berkeley, Berkeley, United States

Lianwen Zhang PhD
Mayo Clinic, Rochester, United States

Tiesuo Zhao PhD
Xinxiang Medical University, Xinxiang, China

Zhicheng Zhou PhD
University of Washington, Seattle, United States